Gene Therapy (2005) 12, 95–100

www.nature.com/gt

RESEARCH ARTICLE

Gene therapy for human small-cell lung carcinoma by inactivation of Skp-2 with virally mediated RNA interference

H Sumimoto[1], S Yamagata[1], A Shimizu[1], H Miyoshi[2], H Mizuguchi[3], T Hayakawa[4], M Miyagishi[5], K Taira[5] and Y Kawakami[1]

[1]*Division of Cellular Signaling, Institute for Advanced Medical Research, Keio University School of Medicine, Shinjuku-ku, Tokyo, Japan;* [2]*Subteam for Manipulation of Cell Fate, BioResource Center, RIKEN Tsukuba Institute, Tsukuba, Japan;* [3]*Division of Cellular and Gene Therapy Products, National Institute of Health Sciences, Setagaya-ku, Tokyo, Japan;* [4]*National Institute of Health Sciences, Setagaya-ku, Tokyo, Japan; and* [5]*Department of Chemistry and Biotechnology, School of Engineering, The University of Tokyo, Hongo, Tokyo, Japan*

Increase of Skp-2, which is involved in the degradation of cell cycle regulators including p27^{Kip1}, p21 and c-myc, is one of the important mechanisms for dysregulation of cell cycles in various cancers. We applied RNA interference (RNAi) for Skp-2 by using HIV-lentiviral or adenoviral vectors for a human small-cell lung carcinoma cell line with increased Skp-2 to evaluate RNAi strategy for cancer gene therapy. HIV-lentivirus-mediated RNAi for Skp-2 resulted in efficient inhibition of the in vitro cell growth of cancer cells with increased Skp-2 through the increase of p27^{Kip1} and p21, but no significant effect on the growth of cells without high Skp-2 expression. Furthermore, intratumoral administration of adenovirus siRNA vector for Skp-2 efficiently inhibited growth of established subcutaneous tumor on NOD/SCID mice. These results indicate that the Skp-2 RNAi may be a useful strategy for gene therapy of cancers with high Skp-2 expression.

Gene Therapy (2005) **12**, 95–100. doi:10.1038/sj.gt.3302391
Published online 23 September 2004

Keywords: *Skp-2; RNA interference; lentivirus; adenovirus*

Introduction

Dysregulation of cell cycle is one of the important mechanisms for uncontrolled growth in most cancers. p27^{Kip1}, a cyclin-dependent kinase (cdk) inhibitor, inhibits the transition from G1 to S phase by suppressing the activity of a cyclin E/cdk2 complex in the late G1 to S phase.[1] In many cancers, including gastric, breast and colorectal cancers, low expression of p27^{Kip1} was reported to be associated with poor prognosis and highly aggressive nature of the tumors.[2] Since the level of the p27^{Kip1} protein is mainly controlled by ubiquitin–proteosomal proteolysis, enhanced degradation of p27^{Kip1} appeared to be an important mechanism for the reduction of p27^{Kip1} in cancers.[3] Skp-2, a member of the F-box protein family, is a specific substrate-recognition subunit of an SCF ubiquitin–protein ligase complex and is involved in the p27^{Kip1} degradation.[4] Increased expression of Skp-2, accompanied by inverse decrease of p27^{Kip1}, was reported in many cancers, including small-cell lung carcinoma (SCLC),[5] oral squamous cell carcinoma,[6] lymphoma[7] or gastric carcinoma,[2] indicating that Skp-2 may be involved in the tumorigenesis of some cancers with the reduced p27^{Kip1}. The Skp-2 was overexpressed in 44% of primary SCLC with the reduced expression of p27^{Kip1} through the gene amplification in 5p11–13.[5] Yokoi *et al*[5,8] have previously shown that downregulation of Skp-2 in an SCLC cell line with antisense oligonucleotides resulted in the inhibition of *in vitro* cell growth. However, the precise mechanism of growth inhibition by the Skp-2 inactivation remains to be investigated. In this study, we have analyzed the mechanism for the inhibition of tumor cell growth using newly developed HIV and adenoviral vectors expressing the Skp-2 siRNA, which may be useful for the future gene therapy.

Correspondence: Professor Y Kawakami, Division of Cellular Signaling, Institute for Advanced Medical Research, Keio University School of Medicine, 35 Shinanomachi, Shinjuku-ku, Tokyo 160-8582, Japan
Received 13 May 2004; accepted 10 August 2004; published online 23 September 2004

Results

HIV vector-mediated RNA interference (RNAi) for Skp-2 resulted in the inhibition of in vitro cell growth of SCLC cell line with elevated Skp-2 expression

We constructed several HIV vectors expressing siRNAs targeting at the Skp-2 mRNA and analyzed their RNAi effects by determining the Skp-2 protein by Western blot analysis after infecting an SCLC cell line, ACC-LC-172, which has the gene amplification and increased expression of Skp-2. Of these siRNA HIV vectors, we selected two HIV vectors, S2 and S5, which mediated efficient reduction of the Skp-2 protein. We next evaluated effects of the RNAi for Skp-2 on *in vitro* growth of the ACC-LC-172 SCLC cells

by infection of these Skp-2 siRNA HIV vectors and a control siRNA HIV vector for firefly lucifrase (GL3B) whose infection did not affect *in vitro* growth, cell cycle status and amounts of Skp-2 protein of ACC-LC-172 compared to uninfected ACC-LC-172 (data not shown). *In vitro* cell growth of ACC-LC-172 was significantly inhibited when infected with the S5 siRNA HIV vector compared to the control GL3B siRNA HIV vector ($P<0.0001$), although transduction efficiency monitored by GFP-expressing cells was comparable among the infected cells (98.7–99.9%). (Figure 1a). The similar cell growth inhibition was observed in a melanoma cell line, A375mel, with the overly expressed Skp2 (data not shown). *In vitro* growth of ACC-LC-172 infected with the S2 siRNA HIV vector was less inhibited than that with S5 ($P=0.0005$) (Figure 1a), associated with the weaker suppression of Skp-2 and less induction of $p27^{Kip1}$ and p21 compared to S5 (Figure 1b). The decrease of the Skp-2 protein accompanied by the reduction of $p27^{Kip1}$ protein, shown by Western blot analysis of cell lysates at day 9 after the infection, was positively correlated with the inhibition of *in vitro* cell growth (Figure 1a and b). Other cdk inhibitor p21 was slightly elevated in the cells infected with the S2 and S5 siRNA HIV vectors similarly with $p27^{Kip1}$ (Figure 1b). The $p57^{Kip2}$ protein was under the detectable limit in this cell line (data not shown). The Rb protein was not changed after the infection. Cell cycle analysis performed on day 9 after the infection demonstrated decrease of the population in S and G2/M phases in the cells infected with the S5 siRNA HIV vector (44.6%) compared to those infected with the GL3B siRNA HIV vector (57.1%) (Table 1). No significant apoptosis was observed in the infected cells by flow cytometry analysis and DNA fragmentation assays (data not shown). These results indicated that the Skp-2 RNAi inhibited cellular growth of ACC-LC-172 through the increase of both cdk inhibitors $p27^{Kip1}$ and p21. In contrast, *in vitro* growth of 293T cells without the Skp-2 overexpression was less sensitive to the inhibitory effect of the Skp-2 RNAi ($P=0.1835$) (Figure 2a), although similar pattern of changes was observed in the Skp-2 and $p27^{Kip1}$ proteins (Figure 2b). The constitutively low-level expression of the Skp-2 in 293T cells may explain the reason for the 293T resistance to the Skp-2 RNAi (Figure 2c). Similarly, *in vitro* cell growth of SBC-1, an SCLC cell line that lacks detectable Skp-2 expression, was not inhibited by the Skp-2 siRNAs (Figure 2d). Thus, virally mediated Skip2 RNAi does not appear to affect cells with low Skp2 expression.

Less involvement of myc in the inhibition of the ACC-LC-172 cell growth by the Skp-2 RNAi

Since Skp-2 was also reported to act as a transcriptional cofactor for c-myc,[9,10] which is involved in cell cycle progression by mediating the activation of cyclin E–cdk2 and cyclin D–cdk4, promoting the G1/S transition,[11] we evaluated the role of myc in the Skp-2 RNAi-mediated cell growth inhibition of the ACC-LC-172 SCLC cells. Increased myc expression was previously reported in most SCLC[11] and mild myc increase (2.03-fold) was detected in ACC-LC-172 (data not shown).

When a firefly luciferase expression plasmid, whose expression is under the control of human telomerase reverse transcriptase (hTERT) gene promoter containing

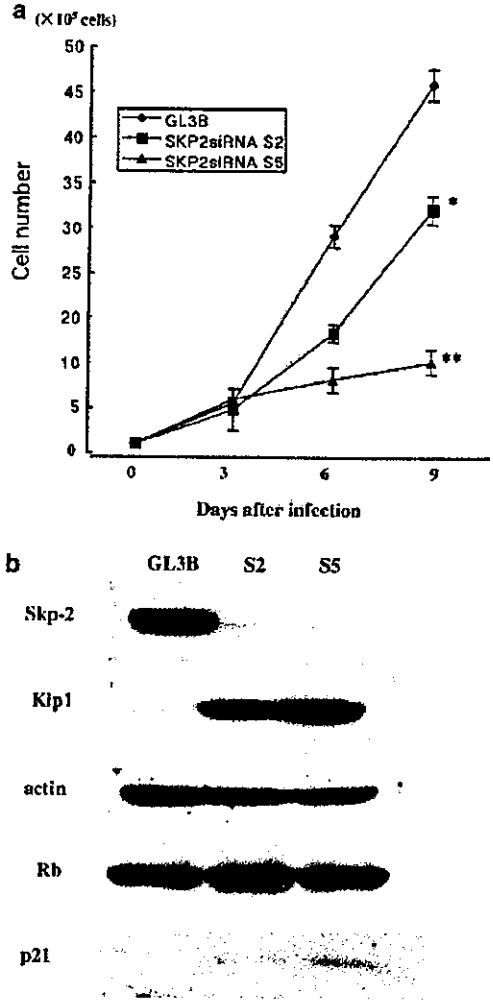

Figure 1 Inhibition of in vitro growth of an SCLC cell line along with decrease of Skp-2 and increase of $p27^{Kip1}$ and p21 by infection of the HIV vectors expressing siRNA for Skp-2: (a) inhibition of in vitro tumor cell growth by virally medicated RNAi for Skp-2. SCLC cell line ACC-LC-172 (100 000) were infected with siRNA HIV vectors for control firefly luciferase (GL3B) or Skp-2 mRNA (S2 and S5) at 100 MOI on day 0, then the cell numbers were determined by trypan blue dye exclusion method on days 3, 6 and 9. The vertical bars indicate the s.d. of the triplicate assays ($P=0.0005$; **$P<0.0001$). This is one representative result of three independent experiments with similar results. (b) Decrease of Skp-2 protein and increase of $p27^{Kip1}$ and p21 proteins by virally medicated RNAi for Skp-2. Cell lysates were prepared from the cells infected with siRNA HIV vectors in (a) on day 9 after the infection. The Skp-2 protein was significantly decreased in cells infected with S2 and S5 compared to GL3B, and $p27^{Kip1}$ and p21 proteins were reciprocally increased in cells infected with S2 and S5. The degrees of the increase of the $p27^{Kip1}$ and p21 proteins were correlated with the degrees of the decrease of the Skp-2 protein. The transduction efficiency determined by GFP expression by flow cytometry was equivalent among the three groups (98.7–99.9%) at the harvest.*

Table 1 Cell cycle status of ACC-LC-172 cells transduced with siRNA HIV vectors for firefly luciferase or Skp-2 mRNAs

siRNA	*% G0/G1*	*% S*	*% G2/M*
GL3B	42.92	45.40	11.68
S2	53.36	31.41	15.23
S5	55.39	35.38	9.23

two myc-binding E-box (CACGTG) motifs[12] (pGL3-hTERT), was transiently transfected to ACC-LC-172, the firefly luciferase activity normalized by *Renilla luciferase* activity was only minimally increased (1.1- to 2.7-fold) compared to that with a pGL3-Basic plasmid (Figure 3),

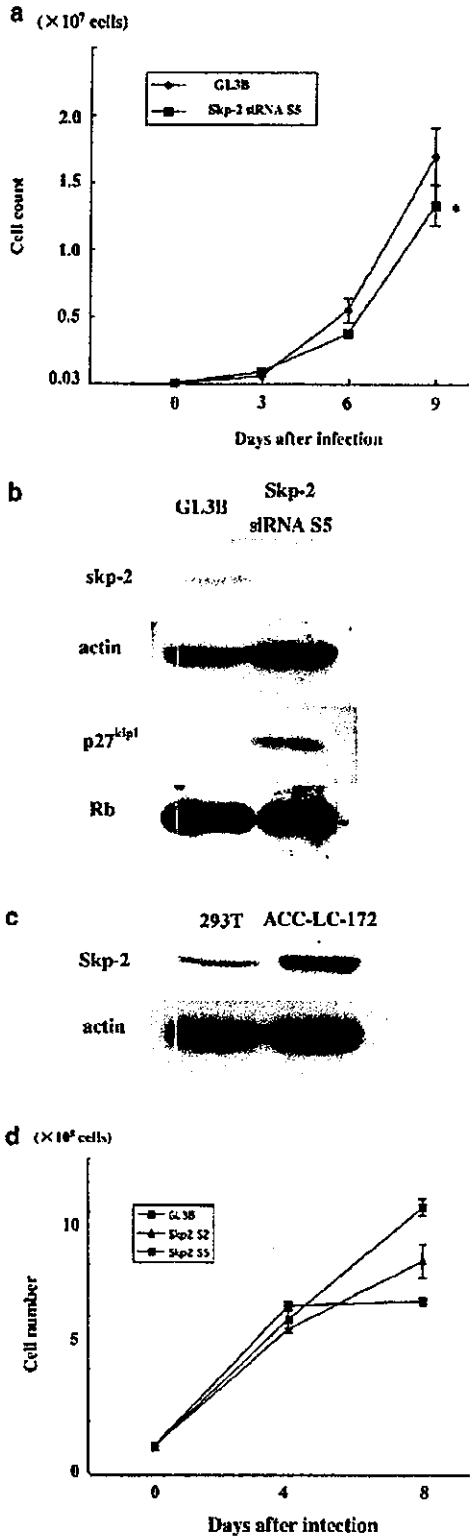

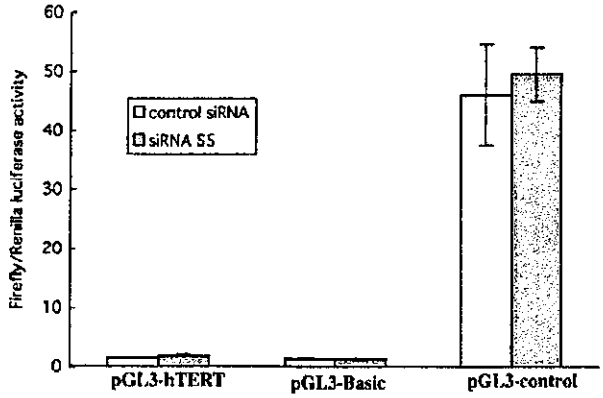

Figure 3 No involvement of myc in the Skp-2 RNAi-mediated cell growth inhibition in the ACC-LC-172 SCLC cell line: ACC-LC-172 cells stably expressing siRNA for Skp-2 (siRNA S5) or control siRNA were transfected with 1 μg of pRL-SV40 (Renilla luciferase expressing plasmid) and 1 μg of pGL3-hTERT, pGL3-Basic or pGL3-control (firefly luciferase expressing plasmids driven by different promoters) by using lipofectamine. At 48 h after the transfection, the cells were harvested and the both Renilla and firefly luciferase activities were determined. Each firefly luciferase activity normalized by the Renilla luciferase activity was calculated. The normalized firefly luciferase activity with pGL3-hTERT was minimally elevated by 1.6-fold compared to with pGL3-Basic without any inhibition in the presence of siRNA for Skp-2. Each bar represents the mean value of triplicate assays and error bars represent the s.d. This is one representative result of three independent experiments with similar results.

suggesting that constitutive myc activity was relatively low in the ACC-LC-172 cells. Transfection of the same plasmid into the ACC-LC-172 cells stably transduced with the HIV Skp-2 siRNA vector (siRNA S5) did not change the luciferase activity. These results indicated that enhancement of myc activity was not the mechanism for the cell growth inhibition of ACC-LC-172 by the Skp-2 RNAi.

In vivo therapeutic activity of intratumoral administration of adenovirus siRNA for Skp-2

To evaluate therapeutic ability of the RNAi for Skp-2, we constructed an adenovirus vector expressing siRNA for

*Figure 2 Minimal inhibition of in vitro growth of 293T cells without increase of Skp-2 expression by infection of the Skp-2 siRNA HIV vectors: minimal inhibition of in vitro growth of 293T cells by the Skp-2 siRNA HIV vector infection. The 293T cells (30 000) were infected with siRNA HIV vectors for control GL3B or Skp-2 mRNA (S5) at 100 MOI on day 0, then the cell numbers were determined as Figure 1a. The vertical bars indicate the s.d. of the triplicate assays (*P = 0.1835). This is one representative result of three independent experiments with similar results. (b) Decrease of the Skp-2 protein and increase of the $p27^{Kip1}$ protein by the Skp-2 siRNA HIV vector infection. Cell lysates were prepared as in Figure 1b. Relatively low expression Skp-2 protein was decreased in cells infected with S5 compared to GL3B, and the $p27^{Kip1}$ protein was reciprocally increased in cells infected with S5, although the changes were less prominent than observed in ACC-LC172 cells. The transduction efficiency determined by GFP expression by flow cytometry was equivalent between the two groups (GL3B: 95.4%; S5: 100.0%) at the harvest. (c) Low expression of Skp-2 in 293T cells compared to ACC-LC-172 SCLC cell line. The amount of the Skp-2 protein was much lower in 293T cells than in ACC-LC-172 cells. The percentage of S+G2/M populations in 293T cells and ACC-LC-172 cells was 74.0 and 58.4%, respectively, at the harvest. (d) SBC-1 SCLC cells lacking detectable Skp-2 were refractory to Skp-2 RNAi. The in vitro cell growth of SBC-1, an SCLC cell line without detectable Skp-2 protein, was not inhibited with Skp-2 siRNA vectors.*

Skp-2, AdF35-Skp-2 siRNA S5, since adenovirus vector is more effective for *in vivo* gene transfer with more efficient production of high-titer viruses. The constructed adenovirus reduced the Skp-2 protein very efficiently in the ACC-LC-172 SCLC cells at only 5 multiplicity of infection (MOI) (Figure 4a), and inhibited the cell growth compared with the control AdF35-GL3B (data not shown). When these adenoviruses were intratumorally injected three times every 2 days to subcutaneously grown ACC-LC-172 SCLC tumors with the largest diameter of 3–4 mm on immunodeficient NOD/SCID mice, growth of tumors injected with the AdF35-Skp-2 siRNA (S5) was significantly reduced compared to that with the control AdF35-GL3B ($P<0.05$) (Figure 4b). These results indicated that Skp-2 is an excellent target for the treatment of cancers with the increased Skp-2, and gene therapy by virally mediated RNAi may be applicable for these cancers.

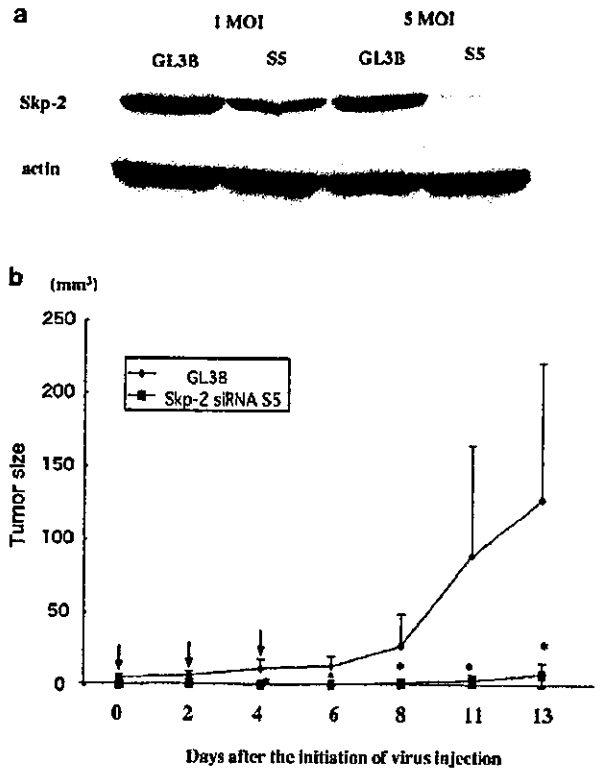

*Figure 4 Inhibition of in vivo tumor growth by intratumoral administration of adenoviral vector expressing siRNA for Skp-2. (a) Efficient downregulation of Skp-2 protein by infection of the Skp-2 siRNA adenoviral vector. Cell lysates from ACC-LC-172 cells infected with AdF35-Skp-2 siRNA S5 or AdF35-GL3B at either 1 or 5 MOI were prepared and analyzed for Skp-2 protein by Western blot analysis. (b) Inhibition of in vivo tumor growth by intratumoral injection of the Skp-2 siRNA. A total of 1×10^8 IFU of AdF35-Skp-2 siRNA S5 ($n=5$) or AdF35-GL3B (control) ($n=4$) were intratumorally injected three times every 2 days as shown in the figure (arrow) to subcutaneously established ACC-LC-172 on NOD/SCID mice. The largest diameter of the tumor reached 3–4 mm when injected with adenoviral vectors. The tumor size was compared between the two groups. *$P<0.05$, the vertical bars indicate s.d.*

Discussion

The cdk inhibitor, $p27^{Kip1}$, controls progression of cell cycles in response to mitogenic stimuli, and is a dosage-dependent tumor suppressor protein.[3] Reduced expression of $p27^{Kip1}$ is not usually caused by genetic change,[3] but often caused by enhanced proteolysis in cancers. The targeted disruption of an ubiquitin–protein ligase Skp-2 resulted in cell cycle arrest in G1 with the accumulation of $p27^{Kip1}$,[13] indicating that Skp-2 regulate cell cycle progression through proteolysis of $p27^{Kip1}$. Patients with cancers with the reduced $p27^{Kip1}$ by increased expression of Skp-2 were reported to have relatively poor prognosis in clinical studies.[6–8]

In this study, we attempted virally mediated RNAi for Skp-2 on the SCLC cell line to analyze the role of Skp-2 in the cell growth as well as to develop possible gene therapy for the Skp-2 overexpressing cancers. The observation that cell growth was inhibited by the virally mediated Skp-2 RNAi, which was accompanied by downregulation of Skp-2 and upregulation of both $p27^{Kip1}$ and p21, indicated that the increased Skp-2 expression is a primary event causing cell cycle progression of the SCLC cell line through the enhanced proteolytic degradation of $p27^{Kip1}$. Interestingly, the degree of the Skp-2 suppression with different siRNAs was correlated with the degree of the elevation of $p27^{Kip1}$ and p21 as well as *in vitro* growth suppression. Although p21 is mainly regulated transcriptionally, Skp-2-mediated ubiquitination and the subsequent proteolysis appear to be involved in the regulation of p21.[14] Although the increase of p21 was not as prominent as that of $p27^{Kip1}$, we also observed significant increase of p21 after the Skp-2 RNAi, indicating that it may also contribute to the cell cycle progression in the SCLC cell line.

Although Yokoi *et al* reported that antisense oligonucleotide-mediated inactivation of Skp-2 resulted in the induction of apoptosis characterized by an increase of the sub-G1 population, fragmentation of nuclei and activation of caspase-3 when evaluated on days 2–4,[8] we did not observe significant increase of the sub-G1 population or DNA fragmentation in the ACC-LC-172 cells with the siRNA HIV vectors in spite of very efficient downregulation of Skp-2 on day 9 (data not shown). This discrepancy may result from the different time point. Remaining on day 9 after the lentiviral infection cells might have been refractory to the apoptotis.

In contrast to the previous reports using Skp-2 $^{-/-}$ mice[13] or forced expression of $p27^{Kip1}$,[1] Skp-2 RNAi did not lead to complete G1 arrest. Although almost complete downregulation of the Skp-2 protein accompanied by the increase of the $p27^{Kip1}$ protein was observed with the siRNA S5 (Figure 1b), these infected cells continued to grow slowly (Figure 1a), possibly due to relative resistance of this cell line to cell cycle inhibition by $p27^{Kip1}$.

In terms of possible use of this strategy for treatment of cancer patients, along with the effective tumor growth inhibition, it should be noted that growth of cells without the increased Skp-2, including 293T cells and primary fibroblasts (data not shown) was hardly affected by Skp-2 RNAi, suggesting that inactivation of Skp-2 is a relatively safe targeting therapy for cancers with high Skp-2 expression. In this study, we also demonstrated

that intratumoral injection of adenovirus vector expressing the Skp-2 siRNA efficiently inhibited *in vivo* growth of the established tumor subcutaneously implanted in NOD/SCID mice, suggesting that viral-mediated Skp-2 RNAi may be applicable for gene therapy. These results altogether indicated that Skp-2 is a good target for gene therapy or other molecular target therapy for patients with cancers expressing high level of Skp-2.

Materials and methods

Cell lines

An ACC-LC-172 cell line (a kind gift from Dr Takahashi, Aichi Cancer Center, Research Institute, Japan) and SBC-1 (purchased from Japanese Collection of Research Bioresources, Japan) established from Japanese patients with SCLC were maintained in RPMI-1640 (Sigma, Japan) supplemented with 10% (v/v) fetal bovine serum, penicillin and streptomycin. The 293T cells were purchased from American Type Culture Collection (ATCC, Manassas, VA, USA) and maintained in DMEM (Sigma, Japan) supplemented with 10% (v/v) fetal bovine serum, penicillin and streptomycin.

HIV vectors

HIV vectors for siRNA expression were constructed from an HIV-U6i-GFP plasmid, which was described previously.[15,16] Briefly, HIV-U6i-GFP has two expression units: one was an siRNA expression cassette, from which a short hairpin RNA was transcribed from human U6 promoter, and the second was a GFP expression cassette, from which GFP gene was transcribed from the CMV promoter. For siRNA expression, *in vitro* annealed complementary oligonucleotides for target sequences were inserted into the two *Bsp*MI sites downstream of the human U6 promoter. Two siRNA target sequences were selected for the Skp-2 RNAi: (S2) ATCA GATCTCTCTACTTTA and (S5) AGGTCTCTGGTGTTT GTAA. Two complementary oligonucleotides, cacc-(target sense)-TTCAAGAGA-(target antisense)-TTTTT and gcatAAAAA-(target sense)-TCTCTTGAA-(target antisense) were synthesized for each target sequence and annealed *in vitro*. The annealed double-stranded (ds) oligonucleotides with 5′-protruding ends complementary to the two *Bsp*MI sites in the HIV-U6i-GFP plasmid were then subcloned into the HIV-U6i-GFP. Control GL3B siRNA (anti-firefly luciferase siRNA) HIV vector was also constructed with the target sequence GTGCGCTGCTGGTGCCAAC. A mutation-specific anti-BRAF siRNA HIV vector (target: GCTACAGA GAAATCTCGATGG) was used for control in a reporter assay. These HIV vectors produce a short hairpin RNA with the linker sequence (TTCAAGAGA) forming a loop structure, then the linker is processed by Dicer, forming a dsRNA that act as an siRNA. The third-generation HIV vectors were produced by transfecting 293T cells with HIV plasmid vectors, pMD.G (VSV-G env expression plasmid), pMDLg/p.RRE (the third-generation packaging plasmid) and pRSV Rev (Rev expression plasmid) (the latter two plasmids were provided by Cell Genesys, USA) by calcium phosphate transfection. The culture supernatants were collected and used as virus stocks after concentration. The viral titer was measured by counting GFP-positive cells after infection on 293T cells.

In vitro growth inhibition assay

ACC-LC-172 cells (100 000) were infected with the siRNA HIV vectors for Skp-2 (S2 or S5) or firefly luciferase (GL3B) at 100 MOI at day 0. Cell numbers were counted every 3 days by trypan blue dye exclusion method until day 9. The 293T cells (30 000) were infected with siRNA HIV vectors for control GL3B or Skp-2 (S5) at 100 MOI at day 0, then the cell numbers were determined every 3 days until day 9. SBC-1 cells (100 000) were infected with the siRNA HIV vectors, S2, S5 or GL3B at 100 MOI. Cell numbers were counted every 4 days until day 8.

Western blot analysis

Cell lysates were prepared in the lysis buffer (20 mM Tris-HCl (pH 7.5), 12.5 mM β-glycerophosphate, 2 mM EGTA, 10 mM NaF, 1 mM benzamide, 1% NP-40, protease inhibition cocktail (complete, EDTA-free (Roche, Germany)) and 1 mM Na_3VO_4) from the infected cells used in *in vitro* growth inhibition assay on day 9 after confirmation of equivalent GFP expression among the groups by flow cytometry. The protein concentration was determined by DC protein assay kit (Bio-Rad, USA). Anti-$p45^{Skp\ 2}$ (Zymed Laboratories Inc., CA, USA), anti-actin (Sigma, USA), anti-$p27^{Kip1}$ (BD Transduction, USA), anti-Rb (Cell Signaling, USA) or anti-p21 (Santa Cruz, USA) Abs was used for the first antibody. An HRP-conjugated anti-IgG antibody was used for the second antibody, and the reaction was detected by chemiluminescence with SuperSignal West Femto Maximum Sensitivity Substrate (Pierce, USA).

Cell cycle analysis

The cells used in the *in vitro* growth inhibition assays were harvested on day 9 and stained with propidium iodide (PI) by using CycleTEST PLUS DNA Reagent Kit (Becton Dickinson, San Jose, CA, USA) according to the manufacturer's instruction. After the stained cells were analyzed by FACSCalibur (Becton Dickinson), the cell cycle status was analyzed with ModFit software (Becton Dickinson).

hTERT reporter construction

A 0.4 kb hTERT promoter sequence was amplified by genomic PCR with the forward primer: CGCTGG GGCCCTCGC TGGCGTCCCT (nts −324 to −300, numbered relative to the translation initiation site); and the reverse primer: CAGCGGCAGCACCTCGCGGTAGTGG (nts +48 to +72). After denaturation for 4 min at 95°C, 27 cycles of denaturation for 1 min at 95°C, annealing for 1 min at 70°C and extension for 1 min at 72°C were performed and followed by completion for 7 min at 72°C. The PCR product was subcloned into a pCRII vector of TA Cloning kit (Invitrogen, San Diego, CA). After the confirmation of the correct sequence, the translation initiation codon was mutated from ATG to TTG by using QuikChange site-directed mutagenesis kit (STRATAGENE, La Jolla, CA, USA). Then, the hTERT promoter was subcloned into a pGL3-Basic vector (Promega, Madison, WI, USA). The resultant construct, pGL3-hTERT, transcribes the firefly luciferase gene under the control of the 0.4 kb hTERT promoter.

Reporter assay

ACC-LC-172 cells (500 000) stably expressing siRNA for Skp-2 (S5) or for BRAF (V599E) (control siRNA specific

for mutated BRAF (V599E) after the infection with HIV vectors) were transfected with 1 μg of *Renilla luciferase* expression plasmid, pRL-SV40 (Promega) and 1 μg of one of the following firefly luciferase expression plasmids: pGL3-hTERT, pGL3-Basic or pGL3-control (Promega) by using Lipofectamine (Invitrogen). At 48 h after the transfection, the cells were harvested and the luciferase activity was analyzed using Dual-Glo Luciferase Assay System (Promega) and a Berthold luminometer. Each firefly luciferase activity was normalized to *Renilla luciferase* activity.

Adenovirus vectors for siRNA

The adenovirus vectors containing Ad5/35 chimeric fiber protein[17] were used in this study. The vector plasmids pAdF35 and the shuttle vector plasmid pHMCMV-GFP1 were described previously.[18] pHMCMV-GFP1 contains the CMV promoter, the GFP gene derived from pEGFP-N1 (Clontech, Palo Alto, CA, USA) and the bovine growth hormone (BGH) poly(A) signal. The siRNA expression unit containing human U6 promoter and two *Bsp*MI cloning sites were excised from the HIV-U6i-GFP plasmid by *Eco*RI digestion, then subcloned into the *Eco*RI site in pHMCMV-GFP1, which was located downstream of the BGH poly(A) signal. This vector was designated as pHMCMV-GFP-U6i. The ds oligonucleotides for the short hairpin RNA can be directly subcloned into the two *Bsp*MI sites of the pHMCMV-GFP-U6i as in HIV-U6i-GFP. Accordingly, the shuttle vector plasmids containing ds oligonucleotides for Skp-2 (S5) or GL3B were constructed. The adenovirus vectors, AdF35-Skp-2 siRNA S5 and AdF35-GL3B, were constructed by an improved *in vitro* ligation method as described.[19] Both adenovirus vectors were propagated in 293 cells and the viral titers were determined using Adeno-X Rpaid Titer Kit (Clontech) according to the manufacturer's instructions.

Animal experiments

Male NOD/SCID mice (6 weeks old) (Japan Clea, Japan) were subcutaneously implanted with 5×10^6 ACC-LC-172 cells. About 1 week after the implantation, when the largest tumor diameter reached about 3–4 mm, we injected 1×10^8 IFU of AdF35-Skp-2 siRNA S5 or AdF35-GL3B into the tumor (day 0). The adenovirus injection was repeated twice every 2 days. The tumor volume (the largest diameter × the perpendicular diameter × the height) was measured every 2 or 3 days until day 13. The animal experimental protocol was approved by the Laboratory Animal Care and Use Committee at Keio University School of Medicine. Mice were treated according to the Guidelines for the Care and Use of Laboratory Animals of Keio University School of Medicine.

Statistical analysis

All statistical analyses were performed according to unpaired Student's *t*-test.

Acknowledgements

We thank Dr M Matsuoka for his helpful discussion and critical review of our manuscript. This work was supported in part by Grant-in-Aid for Scientific Research from the Ministry of Education, Culture, Sports, Science and Technology of Japan, a grant-in-aid for Cancer Research from the Ministry of Health, Labour and Welfare, Japan, for Second Term Comprehensive 10-year Strategy for Cancer Control, the Science Research Promotion Fund from the Promotion and Mutual Aid Cooperation for Private Schools for Japan, and the Keio Gijuku Academic Development Funds.

References

1 Toyoshima H, Hunter T. p27, a novel inhibitor of G1 cyclin–Cdk protein kinase activity, is related to p21. *Cell* 1994; 78: 67–74.
2 Masuda T *et al*. Clinical and biological significance of S-phase kinase-associated protein 2 (Skp2) gene expression in gastric carcinoma: modulation of malignant phenotype by Skp2 overexpression, possibly via p27 proteolysis. *Cancer Res* 2002; 62: 3819–3825.
3 Fero ML *et al*. The murine gene $p27^{Kip1}$ is haplo-insufficient for tumor progression. *Nature* 1998; 396: 177–180.
4 Sutterlüty H *et al*. $p45^{SKP2}$ promotes $p27^{Kip1}$ degradation and induces S phase in quiescent cells. *Nat Cell Biol* 1999; 1: 207–214.
5 Yokoi S *et al*. A novel target gene, SKP2, within the 5p13 amplicon that is frequently detected in small cell lung cancers. *Am J Pathol* 2002; 161: 207–216.
6 Gstaiger M *et al*. Skp2 is oncogenic and overexpressed in human cancers. *Proc Natl Acad Sci USA* 2001; 98: 5043–5048.
7 Latres E *et al*. Role of the F-box protein Skp-2 in lymphomagenesis. *Proc Natl Acad Sci USA* 2001; 98: 2515–2520.
8 Yokoi S *et al*. Down-regulation of SKP2 induces apoptosis in lung-cancer cells. *Cancer Sci* 2003; 94: 344–349.
9 Kim SY *et al*. Skp2 regulates myc protein stability and activity. *Mol Cell* 2003; 11: 1177–1188.
10 Lehr N *et al*. The F-box protein Skp2 participates in c-myc proteosomal degradation and acts as a cofactor for c-myc-regulated transcription. *Mol Cell* 2003; 11: 1189–1200.
11 Zajac-Kaye M. Myc oncogene: a key component in cell cycle regulation and its implication for lung cancer. *Lung Cancer* 2001; 34: S43–S46.
12 Greenberg RA *et al*. Telomerase reverse transcriptase gene is a direct target of c-Myc but is not functionally equivalent in cellular transformation. *Oncogene* 1999; 18: 1219–1226.
13 Nakayama K *et al*. Targeted disruption of Skp2 results in accumulation of cyclin E and $p27^{Kip1}$, polyploidy and centrosome overduplication. *EMBO J* 2000; 19: 2069–2081.
14 Bornstein G *et al*. Role of the SCF^{Skp2} ubiquitin ligase in the degradation of $p21^{Cip1}$ in S phase. *J Biol Chem* 2003; 278: 25752–25757.
15 Miyagishi M *et al*. Optimization of an siRNA-expression system with an improved hairpin and its significant suppressive effects in mammalian cells. *J Gene Med* 2004; 6: 715–723.
16 Sumimoto H *et al*. Inhibition of growth and invasive ability of melanoma by inactivation of mutated BRAF with lentivirus-mediated RNA interference. *Oncogene* 2004; 23: 6031–6039.
17 Mizuguchi H, Hayakawa T. Adenovirus vectors containing chimeric type 5 and type 35 fiber proteins exhibit altered and expanded tropism and increase the size limit of foreign genes. *Gene* 2002; 285: 69–77.
18 Okada N *et al*. Efficient antigen gene transduction using Arg-Gly-Asp fiber-mutant adenovirus vectors can potentiate anti-tumor vaccine efficacy and maturation of murine dendritic cells. *Cancer Res* 2001; 61: 7913–7919.
19 Mizuguchi H, Kay MA. Efficient construction of a recombinant adenovirus vector by an improved *in vitro* ligation method. *Hum Gene Ther* 1998; 9: 2577–2583.

Available online at www.sciencedirect.com
SCIENCE DIRECT®
Biochemical and Biophysical Research Communications 326 (2005) 402–409
BBRC
www.elsevier.com/locate/ybbrc

Constitutively active PDX1 induced efficient insulin production in adult murine liver

Junta Imai[a,b], Hideki Katagiri[b,*], Tetsuya Yamada[a], Yasushi Ishigaki[a], Takehide Ogihara[b], Kenji Uno[a,b], Yutaka Hasegawa[a,b], Junhong Gao[a,b], Hisamitsu Ishihara[a], Hironobu Sasano[c], Hiroyuki Mizuguchi[d], Tomoichiro Asano[e], Yoshitomo Oka[a]

[a] *Division of Molecular Metabolism and Diabetes, Tohoku University Graduate School of Medicine, Japan*
[b] *Division of Advanced Therapeutics for Metabolic Diseases, Center for Translational and Advanced Animal Research, Tohoku University Graduate School of Medicine, Japan*
[c] *Division of Anatomic Pathology, Tohoku University Graduate School of Medicine, Sendai 980-8575, Japan*
[d] *Division of Cellular and Gene Therapy Products, National Institute of Health Science, Tokyo, Japan*
[e] *Department of Physiological Chemistry and Metabolism, University of Tokyo, Tokyo 113-8655, Japan*

Received 21 October 2004
Available online 19 November 2004

Abstract

To generate insulin-producing cells in the liver, recombinant adenovirus containing a constitutively active mutant of PDX1 (PDX1-VP16), designed to activate target genes without the need for protein partners, was prepared and administered intravenously to streptozotocin (STZ)-treated diabetic mice. The effects were compared with those of administering wild-type PDX1 (wt-PDX1) adenovirus. Administration of these adenoviruses at 2×10^8 pfu induced similar levels of PDX1 protein expression in the liver. While wt-PDX1 expression exerted small effects on blood glucose levels, treatment with PDX1-VP16 adenovirus efficiently induced insulin production in hepatocytes, resulting in reversal of STZ-induced hyperglycemia. The effects were sustained through day 40 when exogenous PDX1-VP16 protein expression was undetectable in the liver. Endogenous PDX1 protein came to be expressed in the liver, which is likely to be the mechanism underlying the sustained effects. On the other hand, albumin and transferrin expressions were observed in insulin-producing cells in the liver, suggesting preservation of hepatocytic functions. Thus, transient expression of an active mutant of PDX1 in the liver induced sustained PDX1 and insulin expressions without loss of hepatocytic function.

Keywords: Insulin; PDX1; Gene therapy; Diabetes; Adenovirus; Transdifferentiation

Type 1 diabetes mellitus is characterized by progressive loss of pancreatic β cells, leading to a lifelong dependency on insulin treatments. Recently, marked advances have been made in transplanting pancreatic islets from human cadavers into type 1 diabetics [1]. However, immune rejection and donor supply are still major challenges in islet cell transplantation. In this context, generation of insulin-producing cells by somatic gene therapy may represent a viable alternative for the treatment for diabetes.

The liver is a possible target organ for generation of insulin-producing cells. Pancreatic and hepatic tissues both express several transcription factors such as HNF1α and C/EBPβ. In addition, these tissues also have similar glucose sensing machinery consisting of the GLUT2 glucose transporter and glucokinase. Furthermore, during embryogenesis, the liver and the ventral pancreas appear to arise from the same cell

* Corresponding author. Fax: +81 22 717 8228.
E-mail address: katagiri-tky@umin.ac.jp (H. Katagiri).

0006-291X/$ - see front matter © 2004 Elsevier Inc. All rights reserved.
doi:10.1016/j.bbrc.2004.11.047

population located within the embryonic endoderm [2]. The gene most likely to be responsible for the difference between the liver and pancreas is pancreatic and duodenal homeobox gene 1 (PDX1), also known as IDX1/IPF1/STF1. PDX1 is expressed in pancreatic buds in the endoderm prior to morphological development of the pancreas [3,4] and has been shown to play a fundamental role in regulating pancreatic development. Gene disruption of PDX1 has been shown to inhibit pancreatic bud maturation and outgrowth, resulting in complete absence of the pancreas [5]. In addition, conditional inactivation of PDX1 in insulin-producing cells results in a progressive loss of β cells, suggesting PDX1 to play an essential role in maintaining β cells [6].

Therefore, to generate insulin-producing cells, several groups have overexpressed PDX1 in various sites [7–11]. Adenovirus-mediated transfer of the PDX1 gene reportedly ameliorates streptozotocin (STZ)-induced hyperglycemia in a short time (within 10 days) [7] as well as for longer periods [12] via production of insulin in the liver. However, helper-dependent adenovirus (HDAD)-mediated PDX1 gene transfer into the liver reportedly results in severe hepatitis and functional failure due to production of pancreatic exocrine enzymes [10]. In addition, transgenic mice overexpressing PDX1 in the liver also develop liver failure [11].

PDX1 has been shown to activate target genes by association with several co-factors such as PBX [13] and the expressions of these protein partners are absent in the liver. To produce a version of PDX1 that would activate target genes without the need for protein partners, the VP16 activation domain from herpes simplex virus was fused to the C-terminus of PDX1 (PDX1-VP16). In PDX1-VP16 transgenic *Xenopus* tadpoles, part or all of the liver is converted to pancreatic tissue, while hepatic differentiation products are lost from the regions converted to pancreas [14].

Therefore, in the present study, we prepared PDX1-VP16 adenovirus and compared the effects of PDX1-VP16 expression with those of wt-PDX1 in the adult murine liver in vivo. These recombinant adenoviruses were administered at a titer of 2×10^8 pfu, which is one to two orders of magnitude lower than those used in previous reports [7,12]. Herein we demonstrate PDX1-VP16 gene transduction to induce hepatocytic production of insulin, but not glucagon or amylase, more efficiently than wt-PDX1, resulting in reversal of STZ-induced hyperglycemia. We found that PDX1-VP16 gene therapy induced endogenous PDX1 expression in the liver, and hence sustained expression of insulin. In contrast to transgenic tadpole experiments, the conversion was partial and liver-specific gene expressions including those of albumin and transferrin were maintained in insulin-producing cells.

Materials and methods

Recombinant adenoviruses. Murine PDX1 cDNA was cloned from a MIN6 cDNA library by PCR. Using PCR, the *ClaI* site was added to murine PDX1 cDNA, which was digested with *ClaI* and subcloned into VP16-N (kind gift from Dr. H. Kanamori) as described [14]. Recombinant adenoviruses containing wt-PDX1 and PDX1-VP16 cDNA were prepared as reported previously [15–17]. LacZ adenovirus was used as a control [18].

Animals. Male C57BL/6N mice were purchased from Clea (Tokyo, Japan), housed in an air-conditioned environment, with a 12-h light-dark cycle, and fed a regular unrestricted diet. Diabetes was induced by intraperitoneal injection of 160–170 mg/kg STZ (Sigma St. Louis, MO) in citrate buffer at 5–6 weeks of age. Blood glucose was determined after a 10 h fast at 6 days after STZ injection; mice with fasting glucose levels of 300–600 mg/dl were used for the experiments. The mice were treated with 2×10^8 plaque-forming units of recombinant adenovirus by systemic injection into the tail vein and killed 40 days after adenovirus injection. Serum insulin concentrations were measured using a rat insulin ELISA Kit Ultra Sensitive (Morinaga, Tokyo, Japan).

Oral glucose tolerance tests. Oral glucose tolerance tests were performed 40 days after adenovirus infusion. Serum glucose levels were determined before, and 15, 30, 60, 90, and 120 min after, administration of oral glucose (1 g/kg body weight).

Immunoblotting. Liver samples were homogenized in buffer (100 mM Tris, pH 8.5, 250 mM NaCl, 1% BP-40, and 1 mM EDTA). Tissue homogenates were centrifuged at 14,000*g* for 10 min at 4 °C. Supernatants including tissue protein extracts (180 μg total protein) were then boiled in Laemmli buffer containing 10 mM dithiothreitol. Aliquots of proteins (15 μg) were subjected to SDS–PAGE. Immunoblot analyses were performed using ECL plus a Western Blotting Detection System Kit (Amersham Buckinghamshire, UK). Antibodies to PDX1 (A-17, Santa Cruz Biotechnology, Santa Cruz, CA) and HSV-1 VP16 (vA-19, Santa Cruz Biotechnology) were commercially obtained.

Immunohistochemistry. Livers of mice were excised 40 days after adenoviral treatment and fixed overnight in 10% paraformaldehyde. Fixed tissues were processed for paraffin embedding and 3 μm sections were prepared. For immunohistochemistry, the streptavidin–biotin (SAB) method was performed using a Histofine SAB-PO kit (Nichirei, Tokyo, Japan) for insulin, glucagon, and amylase, and a MAX-PO kit (Nichirei) for somatostatin, and an EnVision kit/HRP (DAKO, Glostrup, Denmark) for pancreatic polypeptide. Slides were deparaffinized, and then were either autoclaved in citrate buffer for antigen retrieval before being incubated in blocking solution (for amylase, somatostatin, and pancreatic polypeptide detection), or immediately exposed to the blocking solution (for insulin and glucagon detection). For insulin detection, sections were incubated for 18 h at 4 °C with monoclonal antibody against human insulin (Sigma) diluted 1:1000 in PBS. For detection of glucagon, sections were incubated for 18 h at 4 °C with antiserum raised against human glucagon (DAKO) diluted 1:3000 in PBS. For detection of somatostatin, sections were incubated overnight at 4 °C with rat anti-somatostatin monoclonal antibody (Chemicon, Temecula, CA) diluted 1:100 in PBS. For detection of pancreatic polypeptide, sections were incubated overnight at 4 °C with antiserum raised against rat pancreatic polypeptide (LINCO, St. Charles, MO) diluted 1:100 in PBS. For detection of amylase, sections were incubated for 18 h at 4 °C with antiserum raised against the C-terminus of human amylase (Santa Cruz Biotechnology) diluted 1:1000 in PBS. Slides were then incubated with the biotinylated IgG for 1 h and next with peroxidase-conjugated streptavidin for 30 min at room temperature. Finally, immunoreactivity was visualized by incubation with a substrate solution containing 3,3′-diaminobenzidine tetrahydrochloride (DAB).

Fluorescent immunocytochemistry. The 3 μm sections of paraffin-embedded liver were processed as follows. For double staining of

insulin and transferrin or albumin, the sections were incubated overnight with antibodies against insulin and transferrin (goat polyclonal; Santa Cruz Biotechnology) or albumin (rabbit polyclonal; Biogenesis, Kingston, New Hampshire) at 4 °C. Antibodies against insulin, transferrin, and albumin were diluted 1:1000, 1:5000, and 1:5000, respectively, in PBS. For double staining of insulin and transferrin, the sections were then incubated for 1 h at room temperature in a mixture of TRITC-conjugated sheep anti-mouse IgG and FITC-conjugated donkey anti-goat IgG (Jackson Immuno Research, West Grove, PA) diluted 1:1000 in PBS. For double staining of insulin and albumin, the sections were incubated in a mixture of Alexa Fluor 488 goat anti-mose IgG (Molecular Probes, Eugene, OR) and Alexa Fluor 546 goat anti-rabbit IgG diluted 1:1000 in PBS. Sections were observed under a fluorescence microscope (Leica DM RXA, Leica Microsystems, Wetzlar, Germany). The image was analyzed with a Q-fluoro analyzing system (Leica).

Results

To express a PDX1 mutant, in the liver, which is constitutively active without association with protein partners, we prepared a recombinant adenovirus encoding the VP16 activation domain from herpes simplex virus [19,20] fused to the C-terminus of murine PDX1 (PDX1-VP16). For comparison, we also prepared recombinant adenoviruses encoding the wild-type PDX1 (wt-PDX1) and LacZ. These recombinant adenoviruses, at 2×10^8 pfu, were injected intravenously 6 days after STZ administration, when hyperglycemia had already developed; blood glucose levels after a 10 h fast were approximately 400 mg/dl (Fig. 1B). Mice given the LacZ adenovirus were used as controls (LacZ-mice). Systemic infusion of recombinant adenoviruses into mice through the tail vein caused transgene expression primarily in the liver, with no detectable expression in peripheral tissues such as muscle, fat, kidney or brain (data not shown), as reported previously [21].

As shown in Fig. 1A, immunoblotting of hepatic lysates on day 3 after adenoviral administration with anti-PDX1 antibody revealed that ectopic expression of wt-PDX1 or PDX1-VP16 was obtained in the liver. Administration of recombinant adenoviruses at the same titer induced similar levels of PDX1 protein expression.

We next examined the effects of treatment with these adenoviruses on STZ-induced hyperglycemia (Fig. 1B). Administration of wt-PDX1 adenovirus did not significantly decrease fasting blood glucose levels through day 20. Although, interestingly, fasting blood glucose levels were slightly but significantly decreased after day 30 as compared with those in STZ-treated LacZ-mice, administration of wt-PDX1 adenovirus at such a low titer exerted only very small effects in terms of reversal of hyperglycemia.

In contrast, administration of PDX1-VP16 adenovirus more effectively reversed STZ-induced hyperglycemia (Fig. 1B). Hepatic expression of PDX1-VP16 induced significant, profound decreases in fasting blood glucose levels. Although fasting blood glucose levels rose slightly between day 10 and day 15, the therapeutic effects were sustained throughout the experiments. As shown in Table 1, some variation in results was observed. Thirteen percent of PDX1-VP16-mice exhibited almost no decrease in blood glucose levels, although the proportion of these mice was significantly lower than that of wt-PDX1-mice. In contrast, in 27% of PDX1-VP16-mice, fasting blood glucose levels were lower than 200 mg/dl. No such normalization of glucose levels was obtained by wt-PDX1 adenovirus administration (Table 1). Thus, PDX1-VP16 expression in the liver more effectively lowered blood glucose levels and these effects persisted even after adenoviral-mediated gene expression had declined.

To examine the mechanism whereby administration of PDX1-VP16 adenovirus efficiently and persistently lowered blood glucose levels in STZ-treated mice, liver sections from these mice on day 40 after adenoviral administration were immunostained with anti-insulin antibody (Fig. 1C). No insulin staining was detectable in the livers of LacZ-mice. In wt-PDX1-mice, very faint staining with anti-insulin antibody was detected in the liver. In contrast, in PDX1-VP16 mice, strong insulin staining was detected in the cytoplasm of hepatocytes in scattered portions of the liver. The insulin positive cells were seen mostly around vessels. The scant residual insulin-positive cells in the pancreas did not differ significantly among these mice (data not shown). Thus, insulin secretion from hepatocytes is likely to contribute to lowering blood glucose levels in PDX1-VP16-mice.

To confirm that the hepatocytes were secreting insulin, serum levels of immunoreactive insulin in these mice on day 40 after adenoviral administration were measured. In LacZ-mice, STZ treatment induced severe insulinopenia: fasting serum insulin levels were less than 40 pg/ml (Fig. 1D), resulting in severe hyperglycemia. Adenoviral administration of the wt-PDX1 gene slightly increased serum insulin levels. In contrast, PDX1-VP16 adenoviral administration resulted in a substantial increase in serum insulin levels, i.e., more than 6-fold (Fig. 1D). On the other hand, fasting serum insulin levels in the control C57Bl/6N mice of the same age, without STZ treatment, were 340.7 ± 29.9 pg/ml ($n = 6$). Thus, hepatic PDX1-VP16 expression improved fasting serum insulin levels to approximately two-thirds those in normal mice. These data suggest that transient PDX1-VP16 expression in the liver exerted sustained and stronger effects in terms of production and secretion of insulin as compared with wt-PDX1 expression, resulting in the reversal of STZ-induced hyperglycemia.

Oral glucose tolerance tests were performed using LacZ-mice, wt-PDX1-mice, and PDX1-VP16-mice on day 40 (Fig. 2A). STZ-treated LacZ-mice exhibited hyperglycemia: more than 450 mg/dl throughout the

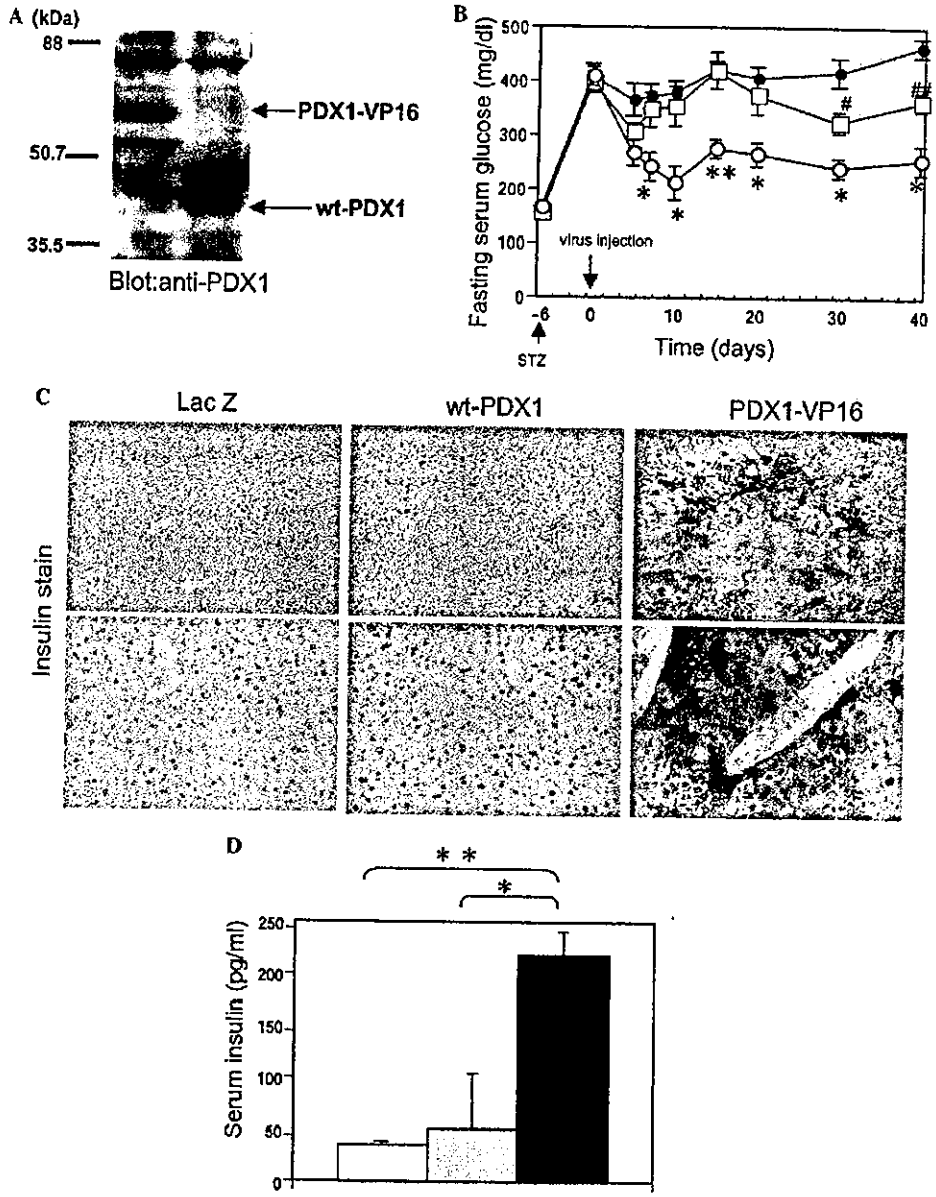

Fig. 1. Effects of wt-PDX1 and PDX1-VP16 adenoviral gene therapy on STZ-induced diabetic mice. (A) Liver lysates from STZ-mice infused with 2×10^8 pfu/body of adenovirus containing wt-PDX1 (left lane) or PDX1-VP16 (right lane) were immunoblotted with anti-PDX1 antibody. (B) Fasting blood glucose levels of STZ-mice treated with LacZ adenovirus (closed circle; $n = 13$), wt-PDX1 adenovirus (open square; $n = 8$) or PDX1-VP16 adenovirus (open circle; $n = 15$). Amount of injected adenoviruses was 2×10^8pfu/body in all experiments. (C) Liver sections from LacZ-mice (left panels), wt-PDX1-mice (middle panels), and PDX1-VP16-mice (right panels) on day 40 after adenoviral treatment were immunostained with anti-insulin antibody. Original magnification 100× (upper panels) and 200× (lower panels). (D) Fasting serum insulin levels 40 days after adenoviral treatment with LacZ (open bar; $n = 7$), wt-PDX1 (gray bar; $n = 8$), or PDX1-VP16 (black bar; $n = 7$) adenovirus. Data are presented as means ± SEM. $^*P < 0.05$, $^{**}P < 0.01$ versus wt-PDX1, $^{\#}p < 0.05$, and $^{\#\#}p < 0.01$ versus LacZ, assessed by unpaired t test.

tests. In PDX1-VP16-mice, glucose levels throughout the tests were significantly lower than those in wt-PDX1-mice. The blood glucose levels peaked at 30 min after glucose load and thereafter tended to fall, although the reversal was incomplete at 120 min. These findings suggest that, in PDX1-VP16-mice, glucose-responsive insulin secretion from the liver is involved in lowering post-prandial blood glucose levels but is not enough to rapidly reverse a rise in blood glucose levels after a glucose load, in contrast to that from the pancreas by β cells.

Using HDAD, PDX1 expression in the liver reportedly induces expression of exocrine enzymes in insulin-producing cells in the liver and causes severe hepatitis. It has also been reported that, in transgenic mice expressing PDX1 ectopically in the liver, not only insulin but

Table 1
Distribution of blood glucose levels in each treatment group

Blood glucose (mg/dl)	100–200	200–300	300–400	400–500	500–600
LacZ (%)	0	0	8	69	23
wt-PDX1 (%)	0	12	50	38	0
PDX1-VP16 (%)	27	47	13	13	0

Blood glucose levels were determined 40 days after each adenoviral treatment. Blood glucose levels of mice before the adenoviral treatment (6 days after STZ injection) were all above 300 mg/dl. (Lac Z; $n = 13$, wt-PDX1; $n = 8$, and PDX1-VP16; $n = 15$.)

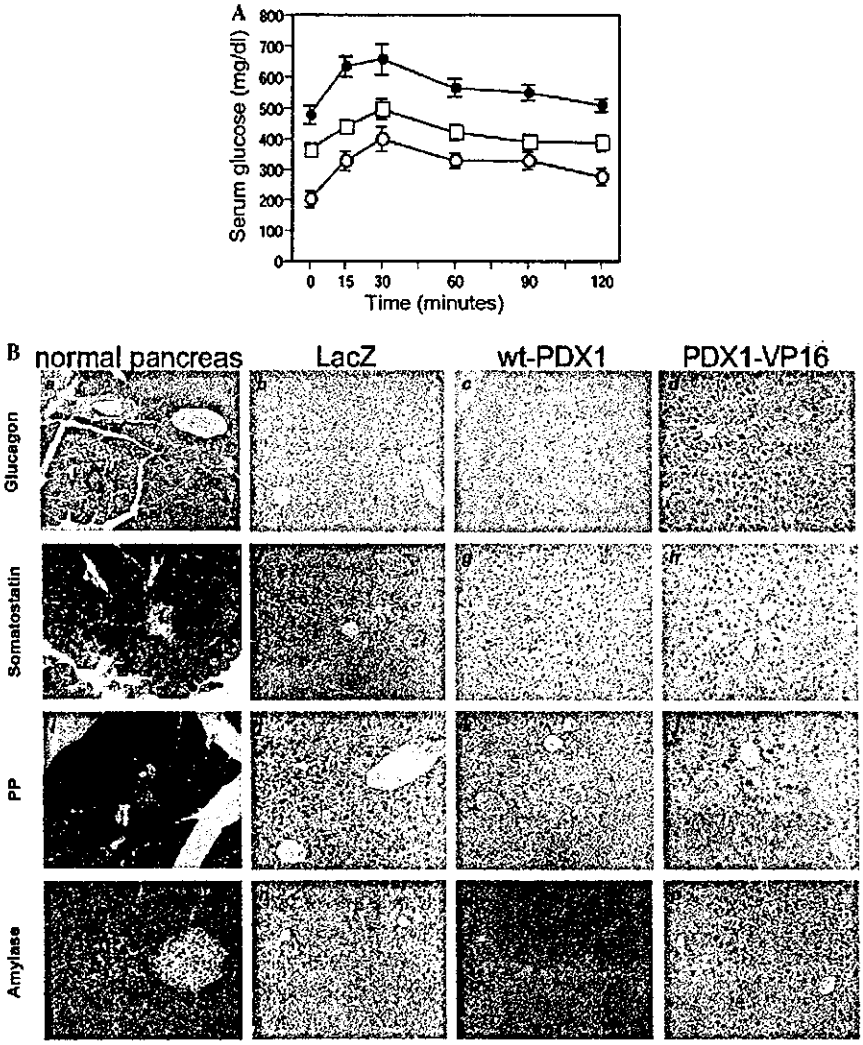

Fig. 2. Effects of wt-PDX1 and PDX1-VP16 adenoviral gene therapy on blood glucose levels after a glucose load, and glucagon, somatostatin, pancreatic polypeptide, and amylase expressions. (A) Blood glucose levels during oral glucose tolerance testing (1 g/kg body weight) in LacZ-mice (closed circle; $n = 7$), wt-PDX1-mice (open square; $n = 8$), and PDX1-VP16-mice (open circle; $n = 7$) on day 40 after adenovirus administration. Data are presented as means ± SEM. (B) immunohistochemical staining of livers from LacZ-mice (b,f,j,n), wt-PDX1-mice (c,g,k,o), and PDX1-VP16-mice (d,h,l,p) with glucagon (b–d), somatostatin (f–h), pancreatic polypeptide (j–l) or amylase (n–p) antibody. Sections of normal pancreas were used as positive controls for each staining procedure (a,e,i,m). Original magnification 100×.

also other endocrine hormones as well as pancreatic exocrine genes are expressed, resulting in dysmorphogenesis and hepatic failure [10]. In contrast, in the present study, adenovirus-mediated transduction of the wt-PDX1 or the PDX1-VP16 gene into the liver did not induce lobe structural abnormalities or substantial infiltration of inflammatory cells (Fig. 2B). Furthermore, using immunohistochemistry, no immunoreactivity against glucagon

or somatostatin was detected in livers from wt-PDX1-mice and PDX1-VP16-mice. In addition, in these livers there was no detectable production of amylase, a pancreatic exocrine enzyme (Fig. 2B), which may explain the normal morphogenesis in our experimental animals. On the other hand, pancreatic polypeptide was expressed in livers from PDX1-VP16-mice, and in those from wt-PDX1-mice though to a lesser extent. These results demonstrate that transient expression of PDX1-VP16 alters the character of hepatocytes to preferentially produce insulin and pancreatic polypeptide, but not other endocrine hormones or exocrine enzymes.

Adenoviral gene transfer induced gene expression for 1 week but, after 2 weeks, this expression reportedly disappeared [22]. However, in the present study, the blood glucose lowering effects and hepatic insulin expression persisted for at least 40 days. Therefore, the time course of PDX1 protein expression levels was examined. As shown in Fig. 3A, immunoblotting using anti-VP16 activation domain antibody revealed PDX1-VP16 protein to be expressed on day 3 but expression was markedly decreased on day 7, and undetectable on day 21. Thus, even after disappearance of VP16-PDX1 expression, hepatocytes expressed insulin, resulting in lowering of blood glucose levels. Interestingly, immunoblotting using anti-PDX1 antibody showed that endogenous PDX1 protein, which had the same molecular weight as wt-PDX1, came to be expressed on day 21. Thus, transient expression of PDX1-VP16 endowed hepatocytes with certain pancreatic β cell features and endogenous PDX1 expression is likely to maintain the insulin-producing function of these cells.

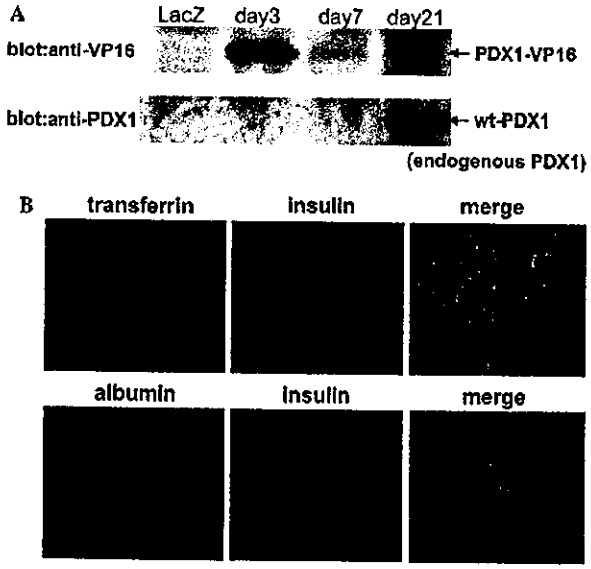

Fig. 3. Treatment with PDX1-VP16 adenovirus induced persistent expression of endogenous PDX1 but albumin and transferrin were co-expressed in insulin-expressing cells. (A) Liver lysates from PDX1-VP16 mice at different time points after adenoviral treatment were immunoblotted with anti-VP16 (upper panel) or anti-PDX1 (lower panel) antibody. (B) Liver sections from PDX1-VP16 mice on day 40 were double-immunostained with insulin (middle panels) and transferrin (upper-left panels) or albumin (lower-left panels) antibodies. Right panels represent the merged images.

To determine whether the insulin-producing cells in the liver had completely transdifferentiated and lost their hepatocytic character, liver sections from PDX1-VP16 mice on day 40 were immunostained with insulin and transferrin (upper panels in Fig. 3B) or albumin (lower panels in Fig. 3B). Fluorescence immunohistochemistry revealed that insulin-producing cells in the liver also expressed transferrin and albumin. Expression levels of these liver-specific proteins were not substantially decreased as compared with non-insulin-producing cells around the insulin-producing cells. These findings suggest functional hepatocyte-specific characteristics are maintained in insulin-producing cells in the liver. Thus, these hepatocytes were not completely converted to pancreatic cells.

Discussion

In the present study, administration of recombinant adenovirus containing an activated form of PDX1 efficiently induced insulin production in hepatocytes, resulting in reversal of STZ-induced hyperglycemia. The effects were sustained even when exogenous protein expression was no longer detectable. In turn, endogenous PDX1 protein came to be expressed in hepatocytes, which is likely to be the mechanism underlying the sustained effects. On the other hand, albumin and transferrin expressions were observed in insulin-producing cells, suggesting the maintenance of hepatocyte-specific characteristics.

Ferber et al. [7] reported that administration of wt-PDX1 adenovirus at 2×10^9 pfu/mouse ameliorates STZ-induced hyperglycemia but the observed period was very short (no more than 10 days). The same research group also reported the long-term effects of PDX1 gene transfer but the titer of recombinant adenovirus used was relatively high ($1–5 \times 10^{10}$ pfu/mouse) [12]. Such high titers may result in liver damage due to adenoviral toxicity. In the present study, to avoid adenoviral toxicity, recombinant adenoviruses were injected at a titer as low as 2×10^8 pfu. With such a small adenoviral delivery, the wt-PDX1 adenovirus exerted very small effects on insulin and glucose levels, whereas PDX1-VP16 adenovirus substantially increased insulin levels and reversed STZ-induced hyperglycemia. These findings suggest that constitutive activation of PDX1 overcomes the inefficiency associated with low expression levels of PDX1 proteins. Thus, adenoviral transfer of the PDX1-VP16 gene into the liver would presumably be safer than wt-PDX1 gene therapy.

HDAD-mediated PDX1 expression in the liver reportedly causes severe hepatitis including marked inflammatory cell infiltration with focal necrosis associated with expression of pancreatic exocrine genes [10]. In addition, conditional transgenic mice generated by crossing CAG-CAT-PDX1 mice with alb-Cre recombinase-mice also displayed functional liver failure with hepatic expression of exocrine enzymes [11]. In these two models, exogenous PDX1 expression is persistent. Transgenes delivered by HDADs are expressed for long periods exceeding several months. In conditional transgenic mice [11], cells, in which the albumin promoter had once been activated, permanently expressed PDX1 driven by the CAG promoter. These findings suggest that high and persistent expression of PDX1 induces exocrine enzyme expression and thereby liver failure. In the present study, exogenous gene expressions of wt-PDX1 and PDX1-VP16 were transient and expression levels were relatively low on day 7 (Fig. 3A). Thus, transient expression appears to be important for endowing hepatocytes with certain features of pancreatic β cells, but not of exocrine cells.

It is noteworthy that exogenous, transient expression of PDX1-VP16 induced prolonged expression of endogenous PDX1 which apparently contributed to persistent insulin production with hepatocytic features. Ber et al. also reported that rat PDX1 gene transduction using first-generation adenovirus induced persistent endogenous (murine) PDX1 expression. Thus, transient expression of wt-PDX1, and more efficiently PDX1-VP16, may induce persistent and low-level expression of endogenous PDX1. In the adult pancreas, persistent but low-level expression of PDX1 is detected only in β cells [3] and PDX1 expression is required for maintaining normal pancreatic β cell function [6]. These observations suggest that persistent, low-level expression of PDX1 is involved in preferential production of insulin and pancreatic popypeptide in hepatocytes.

In transgenic *Xenopus* tadpoles expressing Xlhbox8 (*Xenopus* homolog of PDX1) carrying the VP16 activation domain under a transthyretin promoter, part or all of the liver is reportedly converted to pancreatic tissue without expression of liver-specific gene products, suggesting complete conversion of hepatocytes to pancreatic cells [14]. In contrast, in the present study, insulin-producing cells in the liver in PDX1-VP16 mice also expressed albumin and transferrin, which suggests preservation of hepatocytic functions. This discrepancy may be explained by the differences between amphibian and mammalian cells. Alternatively, the conversion may occur during embryonic differentiation, while, in adult and differentiated hepatocytes, complete transdifferentiation into pancreatic endocrine or exocrine cells would be difficult to achieve even with PDX1-VP16 expression. Although intensive research is necessary to unravel the precise mechanisms underlying transdifferentiation, the partial conversion induced by PDX1-VP16 expression in adult hepatocytes has practical applications, since loss of hepatocytic functions may result in liver failure. Furthermore, incomplete transdifferentiation could prevent the generated insulin-producing cells from being attacked by a destructive autoimmune response in type 1 diabetics.

Acknowledgments

We thank Dr. H. Kanamori (University of Tokyo) for the generous gift of the VP16 gene. We also thank Ms. I. Sato, K. Kawamura, and M. Hoshi for technical support. This work was supported by a Grant-in-Aid for Scientific Research (B2, 15390282), a Grant-in-Aid for Exploratory Research (15659214) to H. Katagiri, and a Grant-in-Aid for Scientific Research (13204062) to Y. Oka from the Ministry of Education, Science, Sports and Culture of Japan. This work was also supported by Tohoku University 21st Century COE Program "CRESCENDO" to J. Imai, J. Gao, and H. Katagiri.

References

[1] A.M. Shapiro, J.R. Lakey, E.A. Ryan, G.S. Korbutt, E. Toth, G.L. Warnock, N.M. Kneteman, R.V. Rajotte, Islet transplantation in seven patients with type 1 diabetes mellitus using a glucocorticoid-free immunosuppressive regimen, N. Engl. J. Med. 343 (2000) 230–238.

[2] G. Deutsch, J. Jung, M. Zheng, J. Lora, K.S. Zaret, A bipotential precursor population for pancreas and liver within the embryonic endoderm, Development 128 (2001) 871–881.

[3] H. Ohlsson, K. Karlsson, T. Edlund, Ipf1, a homeodomain-containing transactivator of the insulin gene, EMBO J. 12 (1993) 4251–4259.

[4] M.F. Offield, T.L. Jetton, P.A. Labosky, M. Ray, R.W. Stein, M.A. Magnuson, B.L. Hogan, C.V. Wright, Pdx-1 is required for pancreatic outgrowth and differentiation of the rostral duodenum, Development 122 (1996) 983–995.

[5] J. Jonsson, L. Carlsson, T. Edlund, H. Edlund, Insulin-promoter-factor 1 is required for pancreas development in mice, Nature 371 (1994) 606–609.

[6] U. Ahlgren, J. Jonsson, L. Jonsson, K. Simu, H. Edlund, Beta-cell-specific inactivation of the mouse ipf1/pdx1 gene results in loss of the beta-cell phenotype and maturity onset diabetes, Genes Dev. 12 (1998) 1763–1768.

[7] S. Ferber, A. Halkin, H. Cohen, I. Ber, Y. Einav, I. Goldberg, I. Barshack, R. Seijffers, J. Kopolovic, N. Kaiser, A. Karasik, Pancreatic and duodenal homeobox gene 1 induces expression of insulin genes in liver and ameliorates streptozotocin-induced hyperglycemia, Nat. Med. 6 (2000) 568–572.

[8] A. Grapin-Botton, A.R. Majithia, D.A. Melton, Key events of pancreas formation are triggered in gut endoderm by ectopic expression of pancreatic regulatory genes, Genes Dev. 15 (2001) 444–454.

[9] R.S. Heller, D.A. Stoffers, M.A. Hussain, C.P. Miller, J.F. Habener, Misexpression of the pancreatic homeodomain protein idx-1 by the hoxa-4 promoter associated with agenesis of the cecum, Gastroenterology 115 (1998) 381–387.

[10] H. Kojima, M. Fujimiya, K. Matsumura, P. Younan, H. Imaeda, M. Maeda, L. Chan, Neurod-betacellulin gene therapy induces islet neogenesis in the liver and reverses diabetes in mice, Nat. Med. 9 (2003) 596–603.

[11] T. Miyatsuka, H. Kaneto, Y. Kajimoto, S. Hirota, Y. Arakawa, Y. Fujitani, Y. Umayahara, H. Watada, Y. Yamasaki, M.A. Magnuson, J. Miyazaki, M. Hori, Ectopically expressed pdx-1 in liver initiates endocrine and exocrine pancreas differentiation but causes dysmorphogenesis, Biochem. Biophys. Res. Commun. 310 (2003) 1017–1025.

[12] I. Ber, K. Shternhall, S. Perl, Z. Ohanuna, I. Goldberg, I. Barshack, L. Benvenisti-Zarum, I. Meivar-Levy, S. Ferber, Functional, persistent, and extended liver to pancreas transdifferentiation, J. Biol. Chem. 278 (2003) 31950–31957.

[13] S. Dutta, M. Gannon, B. Peers, C. Wright, S. Bonner-Weir, M. Montminy, Pdx:Pbx complexes are required for normal proliferation of pancreatic cells during development, Proc. Natl. Acad. Sci. USA 98 (2001) 1065–1070.

[14] M.E. Horb, C.N. Shen, D. Tosh, J.M. Slack, Experimental conversion of liver to pancreas, Curr. Biol. 13 (2003) 105–115.

[15] H. Mizuguchi, M.A. Kay, Efficient construction of a recombinant adenovirus vector by an improved in vitro ligation method, Hum. Gene Ther. 9 (1998) 2577–2583.

[16] H. Mizuguchi, M.A. Kay, A simple method for constructing e1- and e1/e4-deleted recombinant adenoviral vectors, Hum. Gene Ther. 10 (1999) 2013–2017.

[17] T. Anno, S. Uehara, H. Katagiri, Y. Ohta, K. Ueda, H. Mizuguchi, Y. Moriyama, Y. Oka, Y. Tanizawa, Overexpression of constitutively activated glutamate dehydrogenase induces insulin secretion through enhanced glutamate oxidation, Am. J. Physiol. Endocrinol. Metab. 286 (2004) E280–E285.

[18] H. Katagiri, T. Asano, H. Ishihara, K. Inukai, Y. Shibasaki, M. Kikuchi, Y. Yazaki, Y. Oka, Overexpression of catalytic subunit p110alpha of phosphatidylinositol 3-kinase increases glucose transport activity with translocation of glucose transporters in 3t3-l1 adipocytes, J. Biol. Chem. 271 (1996) 16987–16990.

[19] I. Sadowski, J. Ma, S. Triezenberg, M. Ptashne, Gal4-vp16 is an unusually potent transcriptional activator, Nature 335 (1988) 563–564.

[20] S.J. Triezenberg, R.C. Kingsbury, S.L. McKnight, Functional dissection of vp16, the trans-activator of herpes simplex virus immediate early gene expression, Genes Dev. 2 (1988) 718–729.

[21] Y. Ishigaki, S. Oikawa, T. Suzuki, S. Usui, K. Magoori, D.H. Kim, H. Suzuki, J. Sasaki, H. Sasano, M. Okazaki, T. Toyota, T. Saito, T.T. Yamamoto, Virus-mediated transduction of apolipoprotein e (apoe)-sendai develops lipoprotein glomerulopathy in apoe-deficient mice, J. Biol. Chem. 275 (2000) 31269–31273.

[22] M.J. Peeters, G.A. Patijn, A. Lieber, L. Meuse, M.A. Kay, Adenovirus-mediated hepatic gene transfer in mice: comparison of intravascular and biliary administration, Hum. Gene Ther. 7 (1996) 1693–1699.

nature biotechnology

Antibody-targeted cell fusion

Takafumi Nakamura[1], Kah-Whye Peng[1], Sompong Vongpunsawad[1], Mary Harvey[1], Hiroyuki Mizuguchi[2], Takao Hayakawa[3], Roberto Cattaneo[1] & Stephen J Russell[1]

Membrane fusion has many potential applications in biotechnology. Here we show that antibody-targeted cell fusion can be achieved by engineering a fusogenic viral membrane glycoprotein complex. Three different single-chain antibodies were displayed at the extracellular C terminus of the measles hemagglutinin (H) protein, and combinations of point mutations were introduced to ablate its ability to trigger fusion through the native viral receptors CD46 and SLAM. When coexpressed with the measles fusion (F) protein, using plasmid cotransfection or bicistronic adenoviral vectors, the retargeted H proteins could mediate antibody-targeted cell fusion of receptor-negative or receptor-positive index cells with receptor-positive target cells. Adenoviral expression vectors mediating human epidermal growth factor receptor (EGFR)-targeted cell fusion were potently cytotoxic against EGFR-positive tumor cell lines and showed superior antitumor potency against EGFR-positive tumor xenografts as compared with control adenoviruses expressing native (untargeted) or CD38-targeted H proteins.

Cell fusion is essential for fertilization and for the development of placenta, muscle and bone[1]. It provides a basis for stem cell plasticity[2] and is central to the pathogenesis of numerous viral infections[3–5]. Cell fusion is also a scientific tool, used in the production of monoclonal antibodies[6], the identification of oncogenes and tumor suppressor genes[7] and the elucidation of chromosomal functions[8]. Cell fusion has therapeutic applications in cancer gene therapy[9], virotherapy[10] and the generation of novel cancer vaccines[11,12]. We are therefore developing technology to control cell fusion, restricting and redirecting it to achieve target specificity.

Fusion of measles-infected cells is mediated by the viral H and F proteins, which together form a fusogenic membrane glycoprotein complex[3]. The H protein mediates attachment to either one of the viral receptors CD46[13] or SLAM[14] on the cell surface, and signals to the F protein to trigger cell fusion[15]. The steps required to retarget this cell fusion reaction are ablation of H protein–mediated CD46 and SLAM receptor recognition and introduction of a new binding specificity in the H glycoprotein, while preserving its ability to trigger conformational changes in the F protein that lead to membrane fusion. We have demonstrated that single-chain antibodies (scFvs) against carcinoembryonic antigen (CEA) and CD38 (a myeloma cell marker) could be displayed at the C terminus of hybrid H proteins where they triggered F protein–mediated fusion upon binding via the antibody to the targeted receptor[16,17]. However, fusion was also triggered via the natural measles receptors, CD46 and SLAM, which are widely expressed on normal tissues.

We sought to improve target specificity by introducing mutations in the H protein that would block its interactions with CD46 and SLAM. It is known that amino acids 451 and 481 in the H protein play an important role in the interaction with CD46[18]. In addition, by alanine scanning mutagenesis, we recently identified mutations at positions 529 and 533 that ablate fusion through SLAM[19]. We fused an anti-CD38 scFv to the C terminus of the H protein and mutated residues involved in binding to CD46 (451,481) and SLAM (529, 533) (Fig. 1a). Receptor-specific fusion support by the chimeric H protein expression plasmids was determined after F protein–plasmid cotransfection in cells expressing either CD46, SLAM or CD38 (Fig. 1b). Syncytial cytopathic effect was scored by counting syncytia. Paired mutations at positions 451 and 529, or 481 and 533, supported fusion via the targeted CD38 receptor but not via CD46 or SLAM. These data proved conclusively that antibody-targeted cell fusion can be achieved. However, the fusion support activity of the fully retargeted H chimeras on Chinese hamster ovary (CHO)-CD38 cells was considerably lower than that of the original nonablated chimeric protein, H-CD38.

To address the issue of suboptimal fusion support by fully retargeted chimeric H glycoproteins, we focused on residue 481, as amino acid substitutions at this position can have a strong effect on fusion triggering activity[20]. We therefore generated additional H protein chimeras mutated as before at residue 533 (R533A) but with different substitutions at position 481 (Y481M, Y481Q, Y481A) in place of Y481N. Interestingly, all of the new 481-substituted H protein chimeras retained the fully retargeted phenotype but showed higher fusion support activity than the original Y481N mutant on CHO-CD38 cells. In particular, the CD38-targeted chimera carrying mutation Y481A in addition to R533A (H_{AA}-CD38) was slightly more fusogenic on CHO-CD38 cells than was the nonablated chimera H-CD38 (Fig. 1b,c).

Because fusion support activity has been reported to depend on efficient transport and cell surface expression of the H protein[21], we determined total quantities of several chimeric H proteins both in whole cell lysates of transfected cells and at the cell surface (Fig. 1d,e). In CHO-CD38 cells, total cellular H protein expression from the

[1]Molecular Medicine Program, Mayo Foundation, 200 First St. SW, Rochester, Minnesota 55905, USA. [2]Division of Cellular and Gene Therapy Products, [3]National Institute of Health Sciences, Tokyo 158-8501, Japan. Correspondence should be addressed to S.J.R. (sjr@mayo.edu).

Published online 15 February 2004; doi:10.1038/nbt942

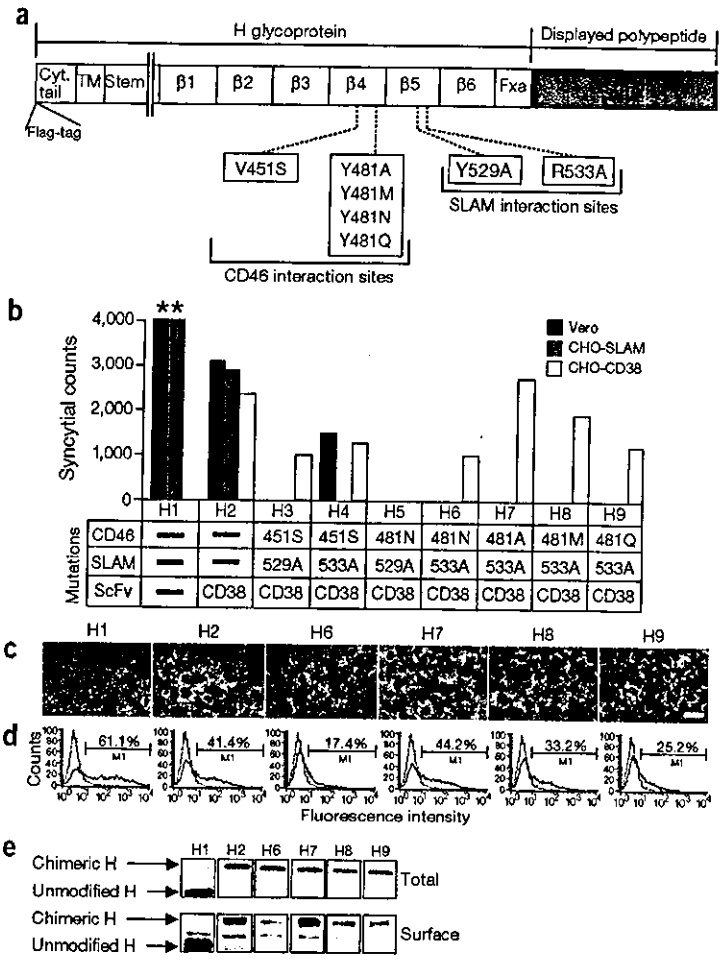

Figure 1 Fusogenic properties of mutant H glycoproteins displaying anti-CD38 antibody. (**a**) Schematic representation of MV-Edm H protein[37] showing H residues mediating CD46 or SLAM interactions. The single-chain antibody is displayed as a C-terminal extension of H glycoprotein and an N-terminal FLAG tag (DYKDDDK) is included to facilitate immunoblot detection. cyt., cytoplasmic; TM, transmembrane; Fxa, Factor Xa cleavage site (IEGR). Standard one-letter abbreviations are used to denote amino acid residues. (**b**) Receptor-specific fusion support by chimeric H expression plasmids after cotransfection with measles F plasmid. Syncytia in five representative fields were counted, and the number of syncytia per well was calculated. Asterisks indicate that the syncytia were not countable because >90% of the cells were in syncytia. (**c**) CHO-CD38 cells were cotransfected with indicated H expression plasmids and measles F, and syncytia were photographed 24 h later. Scale bar, 200 μm. (**d**) Cell surface expression of chimeric H proteins (bold lines), relative to mock transfected cells (thin lines) was determined by FACS analysis after labeling with anti-H antibody. See **b** for H-construct designations. (**e**) Total and cell surface H protein expression levels were also estimated by immunoblotting of cell lysates or of surface biotinylated proteins immunoprecipitated with anti-Flag antibody. See **b** for H-construct designations. The fusogenic activities of the CD38-displaying H chimeras correlate closely with their levels of surface expression.

different chimeric H protein expression plasmids was similar (Fig. 1e). However, cell surface expression, determined by immunoprecipitation of surface biotinylated protein (Fig. 1e) and by fluorescence-activated cell sorting (FACS) analysis (Fig. 1d), differed substantially among the various chimeras. Cell surface expression of every chimeric H protein tested was consistently in accord with the intensity of its fusion support activity on CHO-CD38 cells. In particular, the slightly higher surface expression of the doubly ablated H_{AA}-CD38 mutant in comparison to the nonablated H-CD38 chimera showed that the Y481A and R533A mutations provide the optimal platform for generation of fully retargeted H proteins by scFv display. Indeed, this conclusion was further confirmed by comparing panels of chimeric H proteins displaying alternative scFvs (data not shown).

To determine whether our findings could be generalized to scFvs targeting human cellular receptors other than CD38, we generated doubly ablated (Y481A, R533A) H-protein chimeras displaying C-terminal scFvs recognizing H_{AA}-CEA[16,22] or H_{AA}-EGFR[23]. Each of the doubly ablated, scFv-displaying chimeric H proteins supported fusion, leading to cell death exclusively in cells expressing the relevant targeted receptor (Fig. 2a,b). Background fusion via CD46 or SLAM was not observed. In contrast to these targeted H proteins, the unmodified H protein led to extensive syncytium formation and cytotoxicity in CHO-CD46 and CHO-SLAM cells. Thus, F protein–mediated cell fusion could be fully and accurately redirected through different antibody-receptor interactions by displaying scFvs at the C terminus of a doubly ablated, receptor-blind H protein.

Genes coding for fusogenic membrane glycoproteins have recently been exploited for cytoreductive gene therapy for cancer, whereby transduced cancer cells fuse with neighboring nontransduced cells, leading to tumor regression[9]. To demonstrate the potential of targeted cell fusion for cytoreductive gene therapy of human cancer, we generated bicistronic adenovirus vectors expressing measles F protein with EGFR-targeted, CD38-targeted or untargeted H proteins, and compared their specificity and potency against human ovarian SKOV3ip.1 tumor cells as a treatment model. SKOV3ip.1 cells express low levels of primary coxsackievirus-adenovirus receptor (CAR) and are therefore relatively resistant to adenovirus transduction (Fig. 3a). Adenoviral vectors were therefore used at relatively high multiplicity of infection, standardized to particle counts for all three vectors, to ensure a reasonable efficiency of transduction of ~1% of the tumor cells (Fig. 3b, first panel). The SKOV3ip.1 cells express abundant CD46 and abundant EGFR, but minimal CD38 (Fig. 3a). Surprisingly, in contrast to adenoviruses expressing untargeted measles H protein, the EGFR-targeted adenoviruses could mediate very efficient targeted fusion and killing of SKOV3ip.1 cells. One possible explanation for this difference is that there is a higher absolute density of EGFR compared with CD46 on the SKOV3ip.1 cells. Alternatively, it is possible that the efficiency of F protein triggering by receptor-bound H protein is intrinsically higher

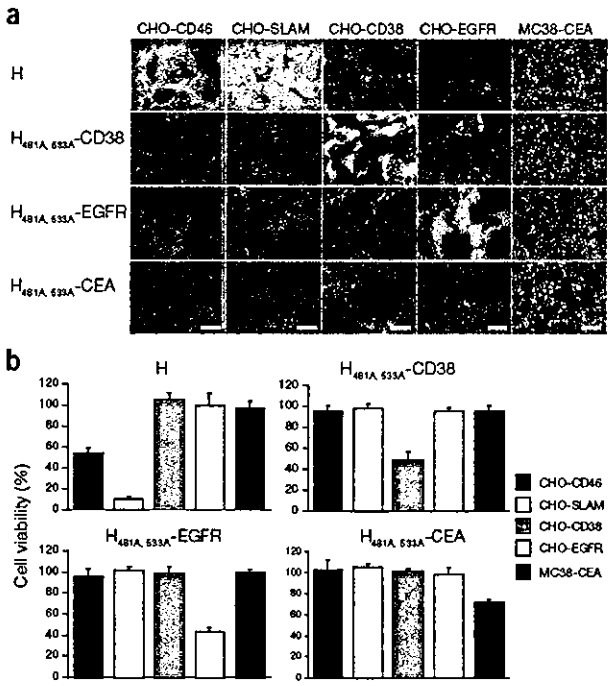

Figure 2 Antibody-targeted cell fusion and cell killing. (**a**) Target cells expressing indicated receptors were cotransfected with indicated H-expression plasmids plus measles F protein, and syncytia were photographed 24 h later. Scale bar, 200 μm. (**b**) Cell viability was determined 36 h after transfection and is shown as the percentage cell survival compared to control mock-transfected cultures. H proteins carrying Y481A and R533A mutations, and displaying cell-targeting scFvs to CD38, EGFR or CEA caused no fusion through CD46 or SLAM receptors, but efficiently mediated targeted cell fusion via CD38, EGFR or CEA, respectively.

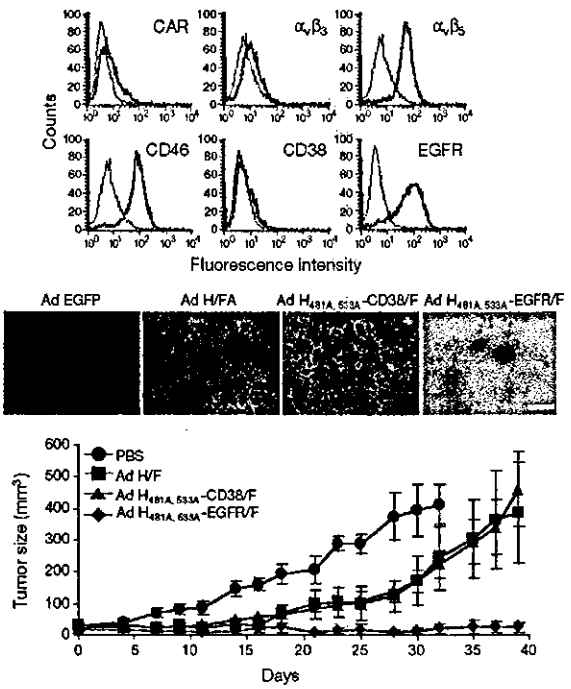

Figure 3 Targeted cytoreductive gene therapy using homologous targeted cell fusion. (**a**) Expression of relevant receptors by human SKOV3ip.1 ovarian tumor cells was determined by FACS analysis. (**b**) Cells were infected with adenoviral vectors expressing EGFP, measles F and H proteins, F protein with CD38-targeted H or F proteins with EGFR-targeted H protein at an MOI of 300 particles/cell. Cells were photographed 48 h after infection. Transduction with adenovirus vectors encoding EGFP is low due to deficiency of CAR. Transduction with the H/F vector led to moderate H/F-induced cell fusion. In contrast, the EGFR-targeted H/F vector caused massive cell fusion and cytotoxicity, whereas the CD38-targeted H/F vector had no effect on these CD38-negative SKOV3ip.1 cells. Scale bar, 200 μm. (**c**) Intratumoral injection of the EGFR-targeted H/F vector elicited potent antitumor effects in contrast to PBS, untargeted H/F and CD38-targeted H/F vectors, and three of six mice in the group showed complete regression.

after binding to EGFR. As expected, control vectors expressing the CD38-targeted H protein showed no fusion activity in SKOV3ip.1 cells.

We next evaluated the *in vivo* effects of these adenoviral vectors against well-established SKOV3ip.1 xenografts implanted subcutaneously in athymic mice. Adenoviral vectors mediating EGFR-targeted fusion showed much greater therapeutic potency in this intratumoral therapy model than control vectors mediating fusion through CD46 (untargeted) or CD38 ($P = 0.0013$ compared to PBS, or $P \leq 0.05$ compared to Ad H/F and Ad $H_{481A, 533A}$-CD38/F; comparisons made on day 32) (Fig. 3c). Histological analysis of explanted tumors 3 d after they were injected with the different adenoviral vectors showed that cell fusion was considerably more prominent in tumors inoculated with vector expressing the EGFR-targeted H protein (data not shown). Taken together, these data demonstrate the superior specificity and potency of vectors mediating antibody-targeted cell fusion in a clinically relevant, cytoreductive, gene therapy model.

Increasingly, cells are exploited as therapeutic agents and antibody-targeted fusion has considerable potential to enhance the therapeutic outcome; stem cells are used for tissue repair, immune effector cells for tumor therapy and vector-modified cells for delivery of diverse genetic payloads[2,24,25]. Recent evidence indicates that stem cell plasticity may be a direct consequence of cell fusion[25] and might therefore be greatly enhanced by directing the stem cells to fuse efficiently with a desired target tissue. Also, heterokaryons obtained by fusing tumor cells with professional antigen-presenting cells (APCs) are known to be potent stimulators of antitumor immunity[11,12]. Antibody-targeted fusion could be used to generate these hybrid cells *in situ* by directing APCs to fuse specifically with tumor cells. Finally, targeted cell fusion provides an appealing strategy to mediate the irreversible trapping of cellular gene delivery vehicles at predetermined target sites.

To demonstrate that heterologous cell fusion between an immune effector cell and an epithelial tumor could be accurately targeted, we infected K562 human erythroleukemic cells with adenoviral vectors expressing nontargeted, EGFR-targeted or CD38-targeted H proteins. K562 cells transduced with the EGFR-targeted or CD38-targeted vector did not fuse with each other but underwent heterologous fusion with EGFR-positive epithelial tumor cells (A431) or with CD38-expressing suspension Jurkat T cells, respectively (Fig. 4a,b). In addition, the EGFR-targeted heterologous fusion was blocked by the presence of anti-EGFR antibody whereas the nontargeted heterologous fusion between K562 and A431 was not (Fig. 4c). An important question arising from these studies relates to the stability of the hybrid cells generated by this method. This is currently under investigation as it is likely to be a key parameter for some of the suggested applications. Our preliminary observation is that the stability of the cell hybrids

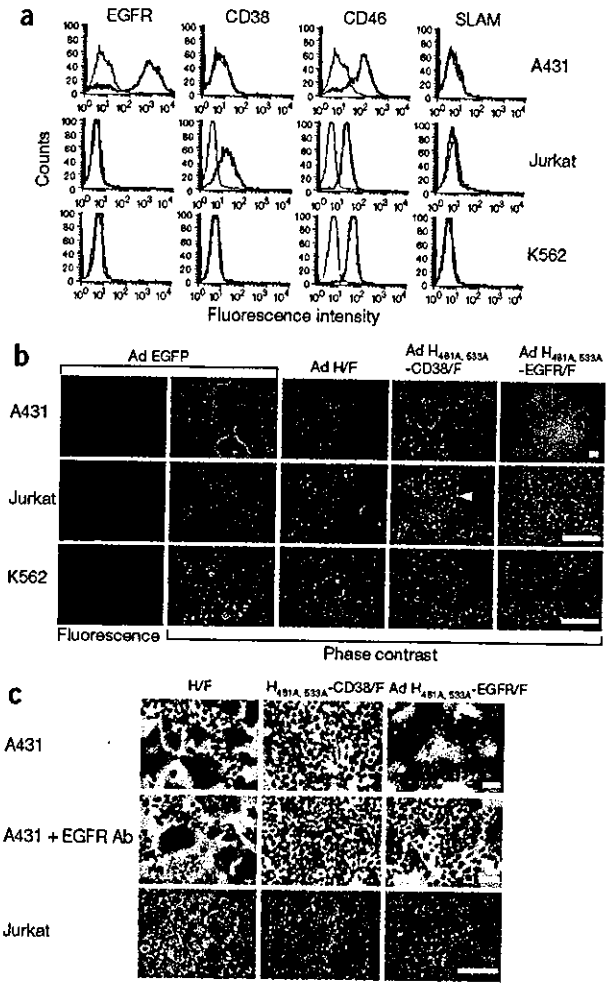

Figure 4 Adenoviral vectors mediating homologous or heterologous targeted cell fusion. (a) Expression of relevant receptors by human tumor cell lines was determined by FACS analysis. (b) Cell lines were infected with adenoviral vectors expressing EGFP, measles F and H proteins, F with CD38-targeted H or F proteins with EGFR-targeted H protein at an MOI of 1,000 particles/cell (for A431) or 10,000 particles/cell (for Jurkat T and K562 cells). Cells were photographed 48 h after infection. Adenovirus vectors encoding CD38 and EGFR-targeted H proteins could mediate targeted fusion and killing of CD38-positive Jurkat T cells or EGFR-positive A431 cells, respectively, but not of receptor-negative K562 cells. The red arrow indicates a syncytium and the white arrow indicates a single cell. (c) However, washed K562 cells expressing CD38 or EGFR-targeted H proteins readily underwent heterologous antibody-targeted cell fusion within 12 h when added to CD38-positive Jurkat T or EGFR-positive A431 cells, respectively. In addition, heterologous EGFR-targeted fusion of adenovirus-infected K562 cells was selectively blocked in the presence of anti-EGFR 528 antibody (EGFR Ab; final concentration 200 ng/ml). Scale bar, 80 μm (b,c).

varies greatly depending upon cell lineage, culture conditions and the number of cell nuclei in each syncytium.

The three cellular receptors targeted in this study belong to widely differing receptor families. CD38 is a 45 kDa type II transmembrane glycoprotein with NAD(P)$^+$glycohydrolase and cell signaling activity[26]; CEA is a heavily glycosylated type I membrane glycoprotein involved in cell adhesion[27]; and EGFR is a type I membrane glycoprotein that undergoes dimerization and rapid endocytosis upon binding EGF[28]. Thus, our data suggest that receptor choice is not a limitation for cell fusion and that it should be possible to target the process through a broad array of cell surface antigens, irrespective of their particular structure. Besides giving insight into the remarkable plasticity of cell fusion triggering mechanisms, antibody-targeted fusion has great potential as a research tool and provides a versatile platform for novel targeted therapies.

METHODS

Cell culture. Vero African green monkey kidney cells (#CCL-81), A431 human epidermoid carcinoma cells (#CRL-1555), Jurkat T-cell leukemia cells (#TIB-152) and K562 human erythroleukemic cells (#CCL-243) were purchased from American Type Culture Collection (ATCC). All cell lines were grown at 37 °C in media recommended by the suppliers in a humidified atmosphere of 5% CO_2. The SKOV3ip.1 ovarian tumor cells were maintained in alpha-MEM (Irvine Scientific) supplemented with 20% (v/v) FBS (Gibco). CHO-CD46 cells were generated by stable transfection of the parental CHO cells using a CD46-C1 isoform expression plasmid[29]. CHO clones stably expressing CD46 were selected using 1.2 mg/ml G418 (Gibco-BRL). Clones expressing high levels of CD46 were identified by flow cytometry using a fluorescein isothiocyanate (FITC)-conjugated, anti-CD46 antibody (Pharmingen). The CHO-CD46 and CHO-CD38[17] cells were grown and maintained in DMEM (Gibco) containing 10% (v/v) FBS, penicillin and streptomycin (DMEM-10) at 37 °C in an atmosphere of 5% CO_2 with 1 mg of G418/ml. CHO-EGFR cells[30] and MC38-cells[31] were grown and maintained in DMEM-10 with 0.5 mg/ml of G418 at 37 °C in an atmosphere of 5% CO_2. CHO-SLAM cells[14] were grown in RPMI 1640 (Gibco) containing 10% FBS, penicillin and streptomycin with 0.5 mg/ml of G418 at 37 °C in an atmosphere of 5% CO_2.

H expression plasmids, transfections and cell fusion assay. Site-directed mutagenesis of pCGHX α-CD38, a measles H glycoprotein expression construct displaying the CD38 scFv[17], was done using the Quick-Change system (Stratagene). Constructs encoding chimeric H proteins with C-terminal scFVs recognizing CEA[22] or EGFR[23] were easily made by exchanging the CD38 scFv fragment via flanking *Sfi*I and *Not*I cloning sites. Cells (8×10^4/well in 24-well plates) were cotransfected with 0.5 μg pCGF, a measles F expression plasmid[32] and 0.5 μg of the appropriate H mutant expression plasmid using Superfect (Qiagen). At 24 h after transfection, the cells were fixed in 0.5% (v/v) glutaraldehyde and stained with 0.1% (w/v) crystal violet, and the syncytia were scored and photographed. For cytotoxicity studies, cells (2×10^4/well in 96-well plates) were transfected with 0.25 μg of pCGF plasmid and 0.25 μg of the appropriate H-protein plasmid, and cell viability was assessed 36 h after transfection using the CellTiter96R Aqueous Non-Radioactive Cell Proliferation Assay (Promega). Results represent means ± s.d. of triplicate determinations.

Surface biotinylation, western blotting and FACS analysis. Cells (4×10^5/well in 6-well plates) were transfected with the appropriate H-protein mutant expression plasmids. After 24 h, the transfected cells were washed two times with 1 ml of ice-cold PBS, and surface proteins were labeled with biotin-7-*N*-hydroxysuccinimide ester for 15 min at 20 °C using a Cellular Labeling kit (Roche). The reaction was stopped by adding NH_4Cl (final concentration, 50 mM) for 15 min at 4 °C. The cells were then washed once, and treated with 500 μl of lysis buffer (50 mM Tris, pH 7.5, 1% (v/v) Igepal CA-630 (Sigma), 1 mM EDTA, 150 mM NaCl, protease inhibitor cocktail (Sigma)) for 15 min at 4 °C, and the lysates were subjected to centrifugation at 4 °C for 15 min at 12,000*g*. Then 20 μl of the resulting postnuclear fraction was directly mixed with an equal volume of SDS loading buffer (130 mM Tris, pH 6.8, 20% (v/v) glycerol, 10% (v/v) SDS, 0.02% (w/v) bromophenol blue, 100 mM dithiothreitol). These samples (40 μl) were denatured for 5 min at 95 °C, fractionated on a 7.5% SDS-polyacrylamide gel, blotted to polyvinylidene difluoride membranes (Bio-Rad), immunoblotted with anti-Flag M2 antibody conjugated to horseradish peroxidase (Sigma) and developed using an enhanced chemiluminescence kit (Pierce) for detection of total H protein. The biotinylated H proteins were immunoprecipitated with anti-Flag antibodies using an immunoprecipitation kit (Roche). We mixed 50 μl of protein A–coated agarose beads with

350 µl of the postnuclear supernatant and 1 µl of anti-Flag M2 antibody (Sigma), followed by overnight incubation at 4 °C under rotation. The agarose beads were then washed three times before resuspension in 50 µl of loading buffer and boiled for 2 min at 100 °C to elute bound proteins. As described above, the samples (40 µl) were fractionated on an SDS-polyacrylamide gel, blotted to polyvinylidene difluoride membranes, and probed with peroxidase-coupled streptavidin (Roche), followed by detection of surface H protein using an enhanced chemiluminescence kit. Alternatively, the surface expression level of H protein was detected by FACS analysis. Twenty-four hours after transfection of the appropriate H mutant or mock plasmid, cells were washed twice with PBS and resuspended in ice-cold PBS containing 2% (v/v) FBS at a concentration of 10^5 cells/ml. The cells were then incubated for 60 min on ice with 1:150 final dilution of the primary mouse monoclonal ascites antibody recognizing measles H protein (Chemicon). Subsequently, the cells were washed with 2% (v/v) FBS/PBS and incubated for an additional 30 min with 1:150 final dilution of FITC-conjugated goat anti-mouse IgG (Santa Cruz Biotechnology). After washing with 2% (v/v) FBS/PBS, the cells were analyzed by flow cytometry using a FACScan system with CELLQuest software (Becton Dickinson). Expression of relevant receptors in A431, Jurkat T cells and K562 human tumor cells was similarly detected by FACS analysis using anti-EGFR 528 (Santa Cruz Biotechnology), anti-CD38, anti-CD46, anti-SLAM antibodies (Pharmingen), anti-CAR antibody RmcB (ATCC), anti-$\alpha_v\beta_3$ antibody (Chemicon) or anti-$\alpha_v\beta_5$ antibody (Gibco).

Adenoviral vectors. All recombinant adenoviruses were constructed using an *in vitro* ligation method as described previously[33]. H, H_{AA}-CD38, H_{AA}-EGFR or EGFP (Clontech) coding sequences were cloned downstream of a human cytomegalovirus immediate early promoter/enhancer ($P_{CMV\ IE}$) in the pHM5 shuttle vector. The F gene was cloned downstream of the $P_{CMV\ IE}$ in the pHM11 shuttle vector. Expression cassettes were transferred from the pHM5 or pHM11 shuttle vectors into the E1 or E3-deleted regions, respectively, of the adenoviral vector plasmid pAdHM48. Genes encoding H protein and EGFP were cloned into the E1 site and the gene encoding F was cloned into E3. The resulting recombinant adenovirus genomes were transfected into human embryonic kidney (HEK)-293 cells. Because expression of measles F and H proteins causes cell fusion and is toxic to HEK-293 cells, viruses were rescued in the presence of a fusion inhibitory peptide (FIP; Bachem), which blocks F/H-protein mediated fusion[34]. The resulting recombinant adenoviruses were propagated in HEK-293 cells in the presence of FIP peptide, and were purified by CsCl-equilibrium centrifugation as described previously[35]. Purified virion preparations were dialyzed against 10 mM PBS, 10% (v/v) glycerol, and finally stored at –80 °C. Viral particle numbers (particles/ml) were calculated from optical density measurements at 260 nm (OD_{260})[36]. All viruses showed similar physical particle titers of approximately 10^{11} particles/ml: Ad EGFP, 1.41×10^{11}; d H/F, 5.75×10^{11}; Ad $H_{481A,533A}$-CD38/F, 2.59×10^{11}; Ad $H_{481A,533A}$-EGFR/F, 3.20×10^{11}.

In vivo experiments. All experimental protocols are approved by the Mayo Foundation Institutional Review Board and Institutional Animal Care and Use Committee. To establish subcutaneous tumors, 6-week-old athymic nu/nu female mice (Harlan Sprague Dawley) were injected with 5×10^6 tumor cells. When the tumors measured 0.3–0.4 cm in diameter, mice received four intratumoral injections of Ad H/F ($n = 6$), Ad $H_{481A,533A}$-CD38/F ($n = 5$), or Ad $H_{481A,533A}$-EGFR/F ($n = 6$) at 7×10^9 viral particles (total 2.8×10^{10}), on days 0, 1, 3 and 4. Control tumors were injected with an equal volume of PBS only ($n = 5$). Animals were killed at the end of the experiment, when tumor burden reached 10% of body weight or when ulcer was seen in tumor. The tumor diameter was measured three times per week and the volume (product of 0.5 × length × length × width) was calculated as mean ± s.e.m. Statistical analysis was performed by analysis of variance followed by Fisher's test, and $P < 0.05$ was considered to be statistically significant.

ACKNOWLEDGMENTS

We thank C.D. James for CHO-EGFR cells, Y. Yanagi for CHO-SLAM cells, J. Schlom for MC38-CEA cells, E. Vitetta for SKOV3ip.1 cells, J.P. Atkinson for CD46 plasmid, J.A. Lust for CD38 scFv, R. Hawkins for CEA scFv and G. Winter for EGFR scFv. We also thank M.J. Federspiel and R.G. Vile for critical reading of the manuscript. This study is supported by the Mayo Foundation, Harold W. Siebens Foundation and NIH grants CA100634-01 and CA90636-01.

COMPETING INTERESTS STATEMENT

The authors declare that they have no competing financial interests.

Received 17 October; accepted 11 December 2003
Published online at http://www.nature.com/naturebiotechnology/

1. Shemer, G. & Podbilewicz, B. Fusomorphogenesis: cell fusion in organ formation. *Dev. Dyn.* **218**, 30–51 (2000).
2. Holden, C. & Vogel, G. Stem cells. Plasticity: time for a reappraisal. *Science* **296**, 2126–2129 (2002).
3. Griffin, D.E. Measles Virus. in *Fields Virology* (eds: Knipe, D.M. & Howley, P.M.) 1402–1442 (Lippincott Williams & Wilkins, Philadelphia, 2001).
4. Freed, E.O. & Martin, M.A. HIVs and their replication. in *Fields Virology* (eds. Knipe, D.M. & Howley, P.M.) 1971–2042 (Lippincott Williams & Wilkins, Philadelphia, 2001).
5. Cohen, J.I. & Straus, S.E. Varicella-Zoster virus and its replication. in *Fields Virology* (eds. Knipe, D.M. & Howley, P.M.) 2707–2730 (Lippincott Williams & Wilkins, Philadelphia, 2001).
6. Kohler, G. & Milstein, C. Continuous cultures of fused cells secreting antibody of predefined specificity. *Nature* **256**, 495–497 (1975).
7. Dorssers, L.C. & Veldscholte, J. Identification of a novel breast-cancer-anti-estrogen-resistance (BCAR2) locus by cell-fusion-mediated gene transfer in human breast-cancer cells. *Int. J. Cancer* **72**, 700–7005 (1997).
8. Dieken, E.S., Epner, E.M., Fiering, S., Fournier, R.E. & Groudine, M. Efficient modification of human chromosomal alleles using recombination-proficient chicken/human microcell hybrids. *Nat. Genet.* **12**, 174–182 (1996).
9. Galanis, E. *et al.* Use of viral fusogenic membrane glycoproteins as novel therapeutic transgenes in gliomas. *Hum. Gene Ther.* **12**, 811–821 (2001).
10. Peng, K.W. *et al.* Intraperitoneal therapy of ovarian cancer using an engineered measles virus. *Cancer Res.* **62**, 4656–4662 (2002).
11. Guo, Y. *et al.* Effective tumor vaccine generated by fusion of hepatoma cells with activated B cells. *Science* **263**, 518–520 (1994).
12. Bateman, A. *et al.* Fusogenic membrane glycoproteins as a novel class of genes for the local and immune-mediated control of tumor growth. *Cancer Res.* **60**, 1492–1497 (2000).
13. Dorig, R.E., Marcil, A., Chopra, A. & Richardson, C.D. The human CD46 molecule is a receptor for measles virus (Edmonston strain). *Cell* **75**, 295–305 (1993).
14. Tatsuo, H., Ono, N., Tanaka, K. & Yanagi, Y. SLAM (CDw150) is a cellular receptor for measles virus. *Nature* **406**, 893–897 (2000).
15. von Messling, V., Zimmer, G., Herrler, G., Haas, L. & Cattaneo, R. The hemagglutinin of canine distemper virus determines tropism and cytopathogenicity. *J. Virol.* **75**, 6418–6427 (2001).
16. Hammond, A.L. *et al.* Single-chain antibody displayed on a recombinant measles virus confers entry through the tumor-associated carcinoembryonic antigen. *J. Virol.* **75**, 2087–2097 (2001).
17. Peng, K.W. *et al.* Oncolytic measles viruses displaying a single-chain antibody against CD38, a myeloma cell marker. *Blood* **101**, 2557–2562 (2003).
18. Lecouturier, V. *et al.* Identification of two amino acids in the hemagglutinin glycoprotein of measles virus (MV) that govern hemadsorption, HeLa cell fusion, and CD46 downregulation: phenotypic markers that differentiate vaccine and wild-type MV strains. *J. Virol.* **70**, 4200–4204 (1996).
19. Vongpunsawad, S., Oezgum, N., Braun, W. & Cattaneo, R. Selectively receptor-bind measles viruses: Identification of the SLAM-and CD46-interacting residues and their localization on a new hemagglutinin structural model. *J. Virol.* **78**, 302–313 (2004).
20. Xie, M., Tanaka, K., Ono, N., Minagawa, H. & Yanagi, Y. Amino acid substitutions at position 481 differently affect the ability of the measles virus hemagglutinin to induce cell fusion in monkey and marmoset cells co-expressing the fusion protein. *Arch. Virol.* **144**, 1689–1699 (1999).
21. Cattaneo, R. & Rose, J.K. Cell fusion by the envelope glycoproteins of persistent measles viruses which caused lethal human brain disease. *J. Virol.* **67**, 1493–1502 (1993).
22. Chester K.A. *et al.* Phage libraries for generation of clinically useful antibodies. *Lancet* **343**, 455–456 (1994).
23. Kettleborough, C.A., Saldanha, J., Heath, V.J., Morrison, C.J. & Bendig, M.M. Humanization of a mouse monoclonal antibody by CDR-grafting: the importance of framework residues on loop conformation. *Protein Eng.* **4**, 773–783 (1991).
24. Wang, G. *et al.* A T cell-independent antitumor response in mice with bone marrow cells retrovirally transduced with an antibody/Fc-gamma chain chimeric receptor gene recognizing a human ovarian cancer antigen. *Nat. Med.* **4**, 168–172 (1998).
25. Wang, X. *et al.* Cell fusion is the principal source of bone-marrow-derived hepatocytes. *Nature* **422**, 897–901 (2003).
26. Mehta, K., Shahid, U. & Malavasi, F. Human CD38, a cell-surface protein with multiple functions. *FASEB J.* **10**, 1408–1417 (1996).
27. Obrink, B. CEA adhesion molecules: multifunctional proteins with signal-regulatory properties. *Curr. Opin. Cell Biol.* **9**, 616–626 (1997).
28. Carpenter, G. Receptor tyrosine kinase substrates: src homology domains and signal transduction. *FASEB J.* **6**, 3283–3289 (1992).
29. Kemper, C. *et al.* Activation of human CD4+ cells with CD3 and CD46 induces a T-regulatory cell 1 phenotype. *Nature* **421**, 388–392 (2003).
30. Schneider, U., Bullough, F., Vongpunsawad, S., Russell, S.J. & Cattaneo, R.

Recombinant measles viruses efficiently entering cells through targeted receptors. *J. Virol.* **74**, 9928–9936 (2000).
31. Robbins, P.F. *et al.* Transduction and expression of the human carcinoembryonic antigen gene in a murine colon carcinoma cell line. *Cancer Res.* **51**, 3657–3662 (1991).
32. Cathomen, T., Buchholz, C.J., Spielhofer, P. & Cattaneo, R. Preferential initiation at the second AUG of the measles virus F mRNA: a role for the long untranslated region. *Virology* **214**, 628–632 (1995).
33. Mizuguchi, H., Xu, Z.L., Sakurai, F., Mayumi, T. & Hayakawa, T. Tight positive regulation of transgene expression by a single adenovirus vector containing the rtTA and tTS expression cassettes in separate genome regions. *Hum. Gene Ther.* **14**, 1265–1277 (2003).
34. Firsching, R. *et al.* Measles virus spread by cell-cell contacts: uncoupling of contact-mediated receptor (CD46) downregulation from virus uptake. *J Virol.* **73**, 5265–5273 (1999).
35. Kanegae, Y. *et al.* Efficient gene activation in mammalian cells by using recombinant adenovirus expressing site-specific Cre recombinase. *Nucl. Acids Res.* **23**, 3816–3821 (1995).
36. Mittereder, N., March, K.L. & Trapnell, B.C. Evaluation of the concentration and bioactivity of adenovirus vectors for gene therapy. *J. Virol.* **70**, 7498–7509 (1996).
37. Langedijk, J.P., Daus, F.J., & van Oirschot, J.T. Sequence and structure alignment of Paramyxoviridae attachment proteins and discovery of enzymatic activity for a morbillivirus hemagglutinin. *J. Virol.* **71**, 6155–6167 (1997).